

# Deep Learning Multi-Classification Using Chest X-Ray Images

---

A Thesis Paper Presented to the Faculty of the  
College of Engineering, Architecture, and Technology  
Notre Dame of Dadiangas University  
General Santos City

---

In Partial Fulfillment of the Requirements for the Degree of  
Bachelor of Science in Computer Science

By  
Rimpos, Kyle Mark  
Vaea, Steve  
Villamor, Denrey

APRIL 2024

## **ACKNOWLEDGEMENT**

This research has been illuminated by the unwavering support and guidance of many individuals and institutions, without whom this endeavor would not have been possible. It is with great honor and appreciation that we acknowledge those who have played a pivotal role in our success, for their contributions have been invaluable.

First, we extend our deepest gratitude to the Almighty for guiding us throughout this journey, illuminating our path with wisdom and grace.

Our heartfelt appreciation goes to our esteemed thesis adviser, whose invaluable guidance and unwavering support have been instrumental in the fruition of this research endeavor.

To our cherished friends, for their constant encouragement and camaraderie, we are forever grateful.

We also express our sincere appreciation to the College Dean for fostering an environment conducive to scholarly pursuits, together with the NDDU community, providing a platform for intellectual growth and collaboration.

To our parents, for their endless love, support and unwavering belief in our capabilities have been our greatest source of strength. We are eternally grateful for your unwavering faith in us and for instilling in us the values of perseverance and resilience.

Last but not least, we acknowledge ourselves for our diligence, perseverance, and dedication to this endeavor. This research has been a testament to our commitment and hard work, and we take immense pride in the knowledge and skills we have acquired along the way. The challenges we faced have only strengthened our resolve and fueled our passion for learning and growth.

JMJ  
Marist Brothers  
Notre Dame of Dadiangas University  
General Santos City

C E R T I F I C A T E O F A P P R O V A L

This thesis hereto entitled:

**Deep Learning Multi-Classification Using Chest X-Ray Images** prepared and submitted by RIMPOS, KYLE MARK F., VILLAMOR, DENREY M., and VAEA, STEVE S., in partial fulfillment of the requirements for the Degree of Bachelor of Science in Computer Science has been examined and is recommended for acceptance and approval for ORAL EXAMINATION.

Approved by the committee on ORAL EXAMINATION with the grade of **PASSED** on April 20, 2024.

**Ms. Lorelyn F. Adrales, MCS, MBA**

Chair/Adviser

**Mr. Ervin G. Sibonga, MIT**

Panel

**Ms. Aileen Mae B. Coronado, MBA, MIT**

Panel

**Ms. Chyril Concemino, MBA, MIST**

Technical Adviser

Accepted in partial fulfillment of the requirements for the Degree of Bachelor of Science in Computer Science.

**Engr. Shiela Jingle A. Sorino, MEE-CE**

Dean, College of Engineering, Architecture and Technology

## ABSTRACT

Lung diseases and emerging viral threats pose significant global health challenges due to their multifaceted origins, emphasizing the crucial need for accurate diagnostics. Rapid advancements in machine learning, specifically deep learning architectures, have enabled highly accurate automated diagnostic tools for respiratory conditions. This work presents a multi-classification CNN for accurate diagnosis of respiratory conditions using chest X-ray images. Leveraging a dataset of 42,729 images and DenseNet121, it achieved 93% accuracy. Integration of data augmentation, fine-tuning, and regularization enhanced model generalization. Notably, hyperparameter tuning and callback optimization improved performance. The model effectively distinguished COVID-19, pneumonia, and tuberculosis cases with high precision, recall, and F1 scores, despite occasional misclassifications. Despite computational constraints, the study identifies areas for improvement, emphasizing the role of deep neural networks in respiratory disease diagnosis. The proposed model contributes to robust diagnostic tools, potentially improving patient care quality, and efficiency, and reducing healthcare costs through technological innovation.

*Keywords— Chest X-Ray, Deep Learning, Multi-Classification, DenseNet121, Pneumonia, Tuberculosis, COVID-19*

# **Chapter I**

## **INTRODUCTION**

### **The Problem and Its Setting**

From infectious conditions like pneumonia and pulmonary tuberculosis to chronic diseases such as asthma and chronic obstructive pulmonary disease (COPD) to complexities that are introduced by emerging viral threats such as COVID-19 that caused years of isolation to minimize the chances of getting severely ill or dying. Lung diseases account for three of the top six causes of death globally. It not only claimed the lives of 76 million people annually but also left many more with debilitating symptoms and disabilities (Agusti et al., 2022).

In 2019, about 2.5 million people died from pneumonia and a third of those victims were children below 5 years old, which makes it one of the leading causes of death for children (Dadonaite & Roser, 2019). Among Southeast Asian nations, the Philippines has 126 deaths per 100,000 people as of 2017 which makes it the third leading cause of death in the nation for all age groups (Santos, 2021). A report from the World Health Organization highlighted that it is believed that the TB bacteria has infected about 25% of the world's population. The South-East Asian countries accounted for 46% of all new TB cases in 2022, with the African Region coming in second with 23%, and the Western Pacific region with 18%. There are 30 countries with the highest TB burden accounting for around 87% of all new cases of TB, with Bangladesh, China, the Democratic Republic of the Congo, India, Indonesia, Nigeria, and Pakistan. The Philippines is among the countries with high tuberculosis incidence with around 1 million active cases and about 70 deaths daily (Flores et al., 2022). Furthermore, complexities

caused by emerging threats such as COVID-19 had around 750,000,000 cases including nearly 7,000,000 confirmed deaths globally (World Health Organization, 2023). The efficient and accurate diagnosis of lung illnesses stands as of vital importance to immediately start treatment to mitigate the effects it can cause to the lungs.

Medical imaging plays an essential role in diagnosing these diseases, enabling physicians and healthcare professionals to diagnose and treat diverse medical conditions as a safe and non-invasive technique (Ford, 2023). Chest X-rays were very helpful in diagnosing pneumonia in patients exhibiting clinical symptoms of the illness (Rahmati et al., 2015). On the other hand, tuberculosis is diagnosed via chest X-ray (CXR) but is not specific enough as oftentimes radiologic findings are indistinguishable from pneumonia through manual analysis by radiologists and physicians which results in patients not receiving the proper treatment (Ahmed, 2023). Therefore additional tests are required such as acid-fast bacilli (AFB) smear and bacteriological culture tests to confirm the disease (Ryu, 2015). COVID-19 infection is associated with pneumonia as severely ill patients with respiratory symptoms are seen to develop pneumonia and those with mild symptoms do not develop pneumonia (Cleverley et al., 2020) yet the use of RT-PCR is still the standard in diagnosing covid-19 that requires the least 24 hours to produce a result (Islam et al., 2022) which is time-consuming and has a high positive false rate that requires another round of testing.

With the advancements in artificial intelligence (AI) with the use of machine/deep learning models, a lot of studies conducted show promising results in classifying these diseases through CXR. Ahmed used different models of convolutional neural networks (CNN) namely, VGG16 and ResNet18, with the support of a support vector machine

(SVM) to analyze CXR for early detection of pneumonia and tuberculosis had achieved an accuracy of (99.6%) with around 6982 CXR images. The same author also conducted a joint diagnosis of pneumonia, tuberculosis, and COVID-19 CXR images using a CNN multiclass model to classify the three different diseases achieving a (98.72%) accuracy that has the best other state-of-the-art studies. These results highlight the promising technology that can help physicians and health professionals to aid them in diagnosing these different diseases that exhibit the same traits.

The goal of this research is to develop a multi-classification deep learning model with a focus on chest X-ray images used in diagnosing COVID-19, pneumonia, and pulmonary tuberculosis. Using deep learning techniques and the increasingly important applications of artificial intelligence in medical diagnostics permits to improvement of automated multi-classification diagnosis that is efficient, accurate, and reliable. With the mentioned existing challenges in traditional medical diagnosis methods, robust computational models are necessary since they tackle potential human error, time-consuming manual analysis, and the potential to limit the cost of patients for additional tests that are required to confirm their illnesses.

The novelty in this research stands due to its comprehensive dataset consisting of 42,729 chest X-ray images from various reputable online sources categorized into four different classes, a potential multi-classification diagnostic system. The study proposes a pre-trained deep learning convolutional neural network architecture, specifically DenseNet121, as a potential model for multi-classification diagnosis coupled with k-fold cross-validation to ensure a comprehensive assessment of the model's performance across

different subsets of the dataset, enhancing the study's findings and an experimental approach to fine-tune hyperparameters for optimal results.

## **Literature Review**

The literature review explores recent research endeavors that harness the capabilities of machine learning and neural networks for classifying and diagnosing prevalent respiratory illnesses.

### Pneumonia

In their study, Stephen et al. proposed a CNN model for pneumonia classification, training it from scratch on a dataset comprising 5,856 chest X-ray images from pediatric patients aged 1 to 5 years. Through rigorous exploration of data augmentation techniques and ten training iterations, they achieved an average accuracy of (95.31%), with an average validation accuracy of (93.73%). Ayan and Ünver pursued a similar investigation but opted for pre-trained models—Xception and VGG16. Their focus on pneumonia diagnosis revealed VGG16 achieving (87%) accuracy, while Xception reached (82%). Despite the lower accuracy, the study emphasized that each neural network has its strengths, with Xception proving more successful than VGG16 with the same dataset.

Yue et al. introduced MobileNet, a lightweight CNN architecture, and compared it with ResNet18, ResNet50, VGG19, and a basic CNN for pneumonia detection. With a dataset of 5,216 training images and 624 test images from Kaggle, MobileNet achieved (94.45%), ResNet18 reached (98.8%), ResNet50 achieved (94.34%), VGG19 scored (94.31%), and the basic CNN attained (94%). The authors concluded that mainstream

models demonstrated proficient pneumonia detection capabilities. In another approach, Kundu et al. proposed a computer-aided diagnosis (CAD) utilizing transfer learning with GoogLeNet, ResNet18, and DenseNet121. Trained on the Radiological Society of North America (RSNA) dataset with five folds of testing and training, the models yielded accuracy rates ranging from (86.65%) to (98.81%). Meanwhile, Darici et al. conducted pneumonia classification using CNN and ensemble learning, addressing dataset imbalance with the synthetic minority over-sampling technique (SMOTE). Despite building models from scratch, they achieved a notable (95%) average accuracy for disease detection and a (78%) average accuracy for multiclass classification.

Harsh Bhatt and Manan Shah developed a new Convolutional Neural Network (CNN) using three models with different kernel sizes, integrated using a weighted ensemble method with an adaptable threshold value for flexible diagnostics. The model achieved high recall (99.23%) and f1-score (88.56%) without relying on transfer learning, making it lightweight and suitable for deployment as a diagnostic tool. EfficientNetB0 and DenseNet121, enriched with attention mechanisms to classify pneumonia images accurately, had shown great results. Using pre-trained models and self-attention modules, the network efficiently captures features from X-ray images. The dataset comprises a wide range of chest X-ray images, allowing an in-depth analysis of the model's algorithms and performance. The results demonstrate high accuracy (95.19%), precision (98.38%), recall (93.84%), F1 score (96.06%), specificity (97.43%), and AUC (0.9564) on the test dataset (An et al., 2024).

## Tuberculosis

Rahman et al. conducted a study using different deep CNN models namely, ResNet18, ResNet50, ResNet101, ChexNet, InceptionV3, Vgg19, DenseNet201, SqueezeNet, and MobileNet, and evaluated their performance with 3500 normal chest X-ray images and 3500 TB infected images. The study also incorporated segmentation that divides the image into distinct and meaningful regions. The results without segmentation in terms of accuracy were, ResNet18 (93.85%), ResNet50 (93.11%), ResNet101 (94.55%), ChexNet (96.47%), InceptionV3 (95.72%), Vgg19 (95.8%), DenseNet201 (95.07%), SqueezeNet (94.18%), and MobileNet (94.33%), results with segmentation are, ResNet18 (96.84%), ResNet50 (97.07%), ResNet101 (97.96%), ChexNet (98.14%), InceptionV3 (98.54%), Vgg19 (97.91%), DenseNet201 (98.6%), SqueezeNet (96.56%), and MobileNet (96.9%), which concludes that segmentation can significantly improve the performance of the classification models.

In another approach, Iqbal et al. proposed a cost-effective and accurate computer-aided diagnosis (CAD) for TB diagnosis that uses the efficient deep learning neural network, TBXNet, which is built using five distinct dual convolutions blocks, each with a different filter size of 32, 64, 128, 256, and 512. The study is conducted with different datasets to differentiate for validation and has achieved an accuracy of (98.98%) which is better than other state-of-the-art methods. A study by Sathirathanacheewin et al. used a pre-trained model to cater to chest X-ray images from two different institutions. The model used is InceptionV3 and the dataset was augmented using color-space, crop-fip, and rotational methods. Each dataset from the two institutions was run separately and has achieved an AUC of (98%) and (85%), respectively. This shows the

distribution shift that resulted in the falling performance of the other dataset due to its poor generalizability.

In another study, Rajakumar et al. focus on implementing an automated scheme for tuberculosis (TB) detection in chest X-ray images using a Deep Learning (DL) approach. The primary goal is to enhance classification accuracy in TB detection. The proposed scheme involves image collection, pre-processing, feature extraction with pre-trained VGG16 and VGG19, optimal feature selection using the Mayfly algorithm (MA), serial feature concatenation, and binary classification with a 5-fold cross-validation. The study evaluates the performance in various scenarios, including conventional and optimal features with VGG16 and VGG19, as well as concatenated dual-deep features (DDF). Experimental results, conducted in MATLAB, demonstrate that the proposed system, especially with DDF, achieves a high classification accuracy of (97.8%) using a K Nearest-Neighbor (KNN) classifier.

Nafisah and Muhammad proposed an automated tuberculosis (TB) detection system using advanced deep learning (DL) models. To address the challenge of dark regions in chest X-ray (CXR) images, which can confuse DL models, sophisticated segmentation networks are employed to extract the region of interest. Segmented images are then inputted into DL models. Various convolutional neural network (CNN) models are tested, with EfficientNetB3 achieving the highest accuracy of (99.1%), a receiver operating characteristic of (99.9%), and an average accuracy of (98.7%). The results confirm that using segmented lung CXR images improves performance compared to using raw images. A recent study by Rahman et al. introduces a novel deep-learning framework that accurately classifies TB, non-TB lung infections, and healthy patients

using a dataset of 40,000 CXR images. Additionally, a machine learning approach diagnoses drug-resistant TB using 3037 CXR images. This study introduces the largest drug-resistant TB dataset and uses a Score-CAM-based visualization technique for model interpretability. The proposed approach achieves (93.32%) accuracy in classifying TB, non-TB, and healthy patients, (87.48%) for drug-resistant vs drug-sensitive TB, and (79.59%) for multi-drug resistant (MDR), extreme drug-resistant (XDR), and sensitive TB classification, surpassing existing literature.

### Covid-19

Ismael and Sengur conducted a study by deep feature extraction through the use support vector machines (SVM) classifier with various kernel functions and trained using 180 covid-19 and 200 normal X-ray images using deep CNN models (ResNet18, ResNet50, ResNet101, VGG16, and VGG19). The best model, ResNet50, achieved an accuracy of (94.7%). Jain et al. incorporated data augmentation, preprocessing techniques, stage-I, and stage-II deep network model designing with 1215 images from online resources that have a final dataset of 1832 images. The study used a 5-fold cross-validation procedure that has produced promising results of (98.93%) accuracy.

Hussain et al. conducted a classification through the use of a novel 22-layer CNN model, CoroDet, and is trained with different publicly available datasets. The study is conducted by classes, the first class for (COVID-19 and normal), the second class for (COVID-19, pneumonia, and normal), and the third class for (COVID-19, viral pneumonia, bacterial pneumonia, and normal). Each class used 5-fold cross-validation that gave the first class an average accuracy of (95.36%), the second class having an

average of (92.76%), and the third class having an average accuracy of (91.76%). Gupta et al. utilized posteroanterior (PA) views of chest X-ray scans from both COVID-19-affected and healthy individuals. After image cleaning and data augmentation, deep learning-based Convolutional Neural Network (CNN) models—specifically Inception V3, Xception, and ResNeXt—were compared for their performance. The dataset consisted of 6432 chest X-ray scans, with 5467 used for training and 965 for validation. The results analysis revealed that the Xception model achieved the highest accuracy at (97.97%) for detecting chest X-ray images compared to other models. Importantly, the study focuses solely on potential methods for classifying COVID-19-infected patients and does not make claims regarding medical accuracy.

In another approach, Bhattacharyya et al. a novel method for detecting COVID-19 and pneumonia in chest X-ray images is proposed. The approach involves a three-step process, starting with the segmentation of raw X-ray images using a conditional generative adversarial network (C-GAN) to obtain lung images. Subsequently, a pipeline combining key point extraction methods and trained deep neural networks (DNN) is employed for feature extraction. Various machine learning (ML) models are then utilized to classify COVID-19, pneumonia, and normal lung images. The highest testing classification accuracy of (96.6%) is achieved with the VGG-19 model associated with the binary robust invariant scalable key-points (BRISK) algorithm. The proposed method, effectively combining DL-based image segmentation and classification architectures, shows promise for efficiently screening COVID-19-infected patients.

## **Theoretical Framework**

The research's progression is outlined in Figure 1 on the following page.

Researchers begin by gathering and integrating various essential datasets from reputable public online resources namely, Kaggle, National Institutes of Health (NIH) through its TB portals program, and additional images from Notre Dame of Dadiangas University Clinic located in General Santos City, Philippines. Once the datasets are gathered, it is followed by data preparation and data preprocessing to categorize different chest X-ray classifications and preparation for training.

The training and validation phase employs a validation strategy named, K-fold cross-validation, a strategy to assess the robustness of the model in performing training and validation in different subsets of the dataset. A k-value of 5 is utilized, partitioning the datasets in an 80/20 split for training and validation subsets, respectively, within each fold. Data augmentation includes a variety of techniques to be applied to enhance the model's capability to generalize unseen data.

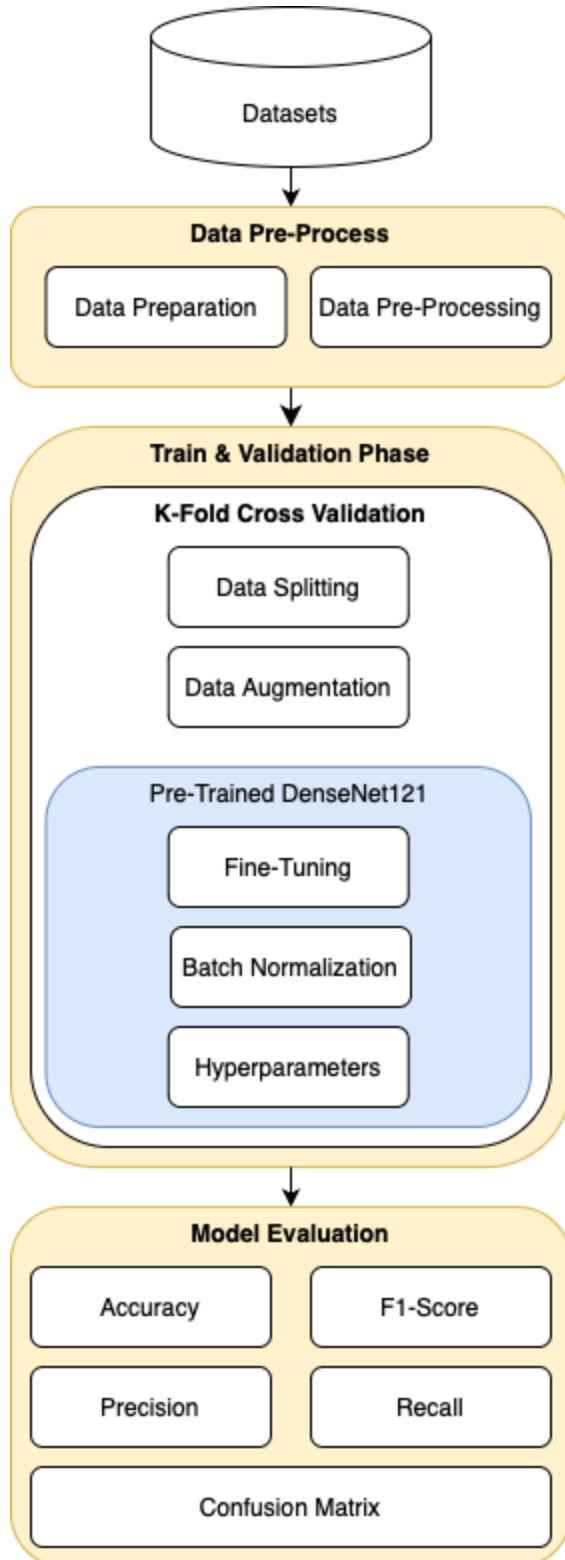


Figure 1. Theoretical Framework

The chosen network architecture, DenseNet121, a widely acclaimed and extensively utilized model for image classification tasks, pre-trained on a large-scale dataset, is leveraged for its proven efficacy. Furthermore, the model will undergo a meticulous fine-tuning process, aligning its parameters with the specific nuances of the dataset, coupled with an experimental hyperparameter tuning procedure to optimize its performance and ensure domain-specific adaptation.

The evaluation phase employs crucial metrics such as the confusion matrix, F1-score, accuracy, recall, precision, and AUROC Curve to comprehensively assess the model's performance. This comprehensive evaluation framework ensures a thorough understanding of the model's capability to classify medical images.

### **Statement of The Problem**

The primary objective of this research is to develop a deep convolutional neural network (CNN) for classifying pneumonia, pulmonary tuberculosis, and COVID-19 chest X-ray images. Specifically, the study aims to address the following objectives:

1. Collect and classify chest X-ray images of the following diseases:
  - 1.1. Pneumonia
  - 1.2. COVID-19
  - 1.3. Pulmonary Tuberculosis
  - 1.4. Normal
2. Identify and apply various data augmentation techniques.
3. Determine the pre-trained model and hyperparameters.

4. Evaluate the performance of the model in each fold, classifying chest X-ray images of pneumonia, pulmonary tuberculosis, and COVID-19 in terms of:
  - 4.1. Accuracy
  - 4.2. Precision
  - 4.3. Recall
  - 4.4. F1- Score
  - 4.5. Confusion Matrix

## **Scope and Delimitation**

The primary objective of this research endeavor is to develop a multi-classification model for distinguishing pneumonia, tuberculosis, COVID-19, and normal cases using a deep convolutional neural network (CNN), specifically, DenseNet121.

The scope encompasses machine learning operations such as data collection, data preparation, data pre-processing, training and validation, and model evaluation. Data collection will only be limited to accurately labeled datasets from reputable public online resources, together with additional images from Notre Dame of Dadiangas University Clinic. Data Preparation and Data Preprocessing are also limited specifically to cater to the study and network's architecture requirements.

The training and validation phase focuses on the study's framework, dataset splitting, data augmentation, training, and validation using a pre-trained model, DenseNet121 paired with fine-tuning and hyperparameters-tuning to optimize model performance for better convergence. Evaluation metrics such as accuracy, precision,

recall, and confusion matrix analysis are utilized to assess the model's classification efficacy.

However, acknowledging the limitations of this research is of utmost importance which includes dataset biases due to uneven distribution of classes. Additionally, variations in imaging protocols across different healthcare institutions are taken into account which does not represent the global diversity of chest X-ray images.

Furthermore, the research may need to address the clarity of how the model makes decisions, ethical considerations regarding AI in healthcare, and challenges in deploying the system including integration with current clinical systems and ensuring compliance with regulations.

### **Significance of the Study**

This study will be beneficial to the following:

**Patients.** Improved and timely diagnosis leads to more effective interventions and treatments, reducing the need for additional costly tests and alleviating financial burdens. It also enhances overall patient outcomes and quality of life.

**Healthcare Professionals.** Reduced manual workload and optimized workflows allow professionals to focus on complex cases and individualized patient care, enabling quicker decision-making and initial screening. This improves healthcare efficiency and effectiveness.

**Limited Access Areas.** Communities with limited access to healthcare facilities benefit from a cost-effective diagnostic system, improving healthcare accessibility in underserved areas and reducing disparities in healthcare delivery.

**Medical Research.** The study contributes new knowledge and insights to medical research, particularly in the integration of medical imaging and artificial intelligence. This fosters innovations in disease diagnosis and treatment methods.

**Public Health.** Early detection systems without costly tests help public health initiatives mitigate and control the spread of diseases more effectively. This can lead to improved public health outcomes and reduced healthcare burdens.

**Communities.** Accurate disease detection leads to early intervention and treatment, reducing the exposure of communities to various lung diseases. This promotes community well-being and contributes to overall public health.

**Financially Challenged Individuals.** By reducing the need for expensive tests and interventions, this study has the potential to lower overall healthcare costs and improve the economic well-being of individuals. It can also stimulate economic growth through improved productivity and reduced healthcare spending.

## **Chapter II**

### **METHODOLOGY**

This chapter introduces the research design, research instruments, selection of the respondents, data gathering procedure, data analysis, and ethical considerations taken into account.

#### **Research Design**

The research employs a quantitative-experimental design that uses feature selection and machine learning classification techniques. The goal of quantitative research is to collect data through measurements, examine those data for trends and relationships, and then validate the measurements taken (Roger, 2015). Machine learning articles use experimental research design as it involves designing an experiment and how to experiment to acquire results through data collection, data pre-processing, model training, model testing, and model evaluation (Kamiri, 2021).

The research design is suitable for this research study as it is focused on classifying chest X-ray images using a deep-learning neural network that will require evaluation metrics to measure the performance of the model quantitatively. Subsequently, the research incorporates additional techniques that will boost the model's performance through data augmentation, fine-tuning, and hyperparameters.

#### **Data Gathering Procedure**

This section enumerates the step-by-step procedures that will be followed in conducting the data-gathering of the research.

1. Researchers gather chest X-ray (CXR) images of pneumonia, tuberculosis, COVID-19, and normal conditions from reputable public online sources and Notre Dame of Dadiangas University's Clinic, ensuring proper citation, obtaining approvals through signed waivers, and drafting a permission letter to the school.
2. Ethical considerations and proper citation for different reference sources are taken into account in handling both the collected data and the literature.

## **Data Analysis**

This section discusses the evaluation metrics used to evaluate the performance of the model in classifying chest X-ray (CXR) images.

### Accuracy

The proportion of correctly predicted data points among all the data points is known as accuracy. The number of true positives and true negatives divided by the total number of true positives, true negatives, false positives, and false negatives is how it is more precisely defined (Tan, 2020).

$$Accuracy = (TP + TN) / (TP + TN + FP + FN)$$

### Recall

The percentage of data samples that a machine learning model correctly classifies as belonging to an interesting class—the "positive class"—out of all the samples for that class is known as recall, also known as the true positive rate (TPR). On top of these

values, machine learning recall is calculated by dividing the true positives (TP) by all of the positive predictions that should have been made (TP + FN).

$$Recall = TP / (TN + FN)$$

## Precision

Precision is the ability of a classification model to isolate only the relevant data elements. Calculating precision in mathematics involves dividing the total true positives by the total true positives plus false positives (Aslan, 2023).

$$Precision = TP / (TP + FP)$$

## F1-Score

An alternative machine learning evaluation metric called the F1-score evaluates a model's predictive ability by focusing on its performance within each class rather than its overall performance as is done by accuracy. A model's precision and recall scores are combined into one metric, the F1 score, which has led to its widespread use in recent literature (Kundu, 2022).

$$F1 - Score = (2 * Precision * Recall) / (Precision + Recall)$$

## Confusion Matrix

The classification performance of a classifier about some test data is summarized by a confusion matrix. It is a two-dimensional matrix with the true class of an object as its index in one dimension and the class the classifier assigns to it in the other (Ting,

2011). The confusion matrix was used to assess how well the methods used after the classification were performed (Bajaj & Sinha, 2022).

TABLE I. CONFUSION MATRIX

		Predicted Class	
		True Positive	False Negative
True Class	True Positive	False Negative	True Negative
	False Positive	True Negative	

### **Ethical Considerations**

In this study, a commitment to various ethical considerations will be taken into account.

**Informed Consent.** Informed consent will be diligently obtained from research participants, ensuring that they fully comprehend the study's purpose, potential risks, and benefits before they voluntarily agree to participate.

**Anonymity.** To protect the identities and personal information of the research participants, rigorous measures will be employed to ensure that all data is collected and stored without any links to specific individuals.

**Confidentiality.** The research will maintain strict confidentiality standards in handling all personal and medical data that will be collected during the duration of the research.

**Plagiarism.** To maintain the accuracy of the findings, originality and accurate citation of sources will be upheld.

**Transparency.** The researchers pledged to be completely transparent in publicly disclosing their research methodologies, conclusions, and potential limitations.

**Privacy.** The research will employ stringent security measures to safeguard private information that will be collected from research participants and ensure that data utilization complies with all applicable privacy laws and moral standards.

## **Chapter III**

### **RESULTS**

This chapter presents the results of the dataset collection, model architecture, and model performance evaluation. Visualizations are provided for further analysis, to be discussed in the subsequent chapter.

#### **Presentation of Data**

##### **Covid-Qu-Ex Dataset**

The dataset utilized in this research is curated by researchers from Qatar University, drawing from publicly accessible datasets online. Specifically, it encompasses contributions from various sources, including the QaTa-Covid19 Dataset, Covid-19-image-repository, Eurorad, Covid-chest x-ray Dataset, Covid-19 Dataset, COVID-19 Radiography Database, Covid-CXNet, RSNA Pneumonia Detection Challenge, Chest X-Ray Images (Pneumonia) Dataset, and Medical Imaging Databank of Valencia Region. Comprising a total of 33, 920 meticulously classified chest X-ray (CXR) images, each accompanied by its respective ground truth lung masks, the dataset encompasses 11, 956 COVID-19 images, 11, 263 cases of Non-COVID infections (Viral or Bacterial Pneumonia), and 10, 702 Normal images. It is publicly accessible via Kaggle for download and serves as the foundational resource for this study.

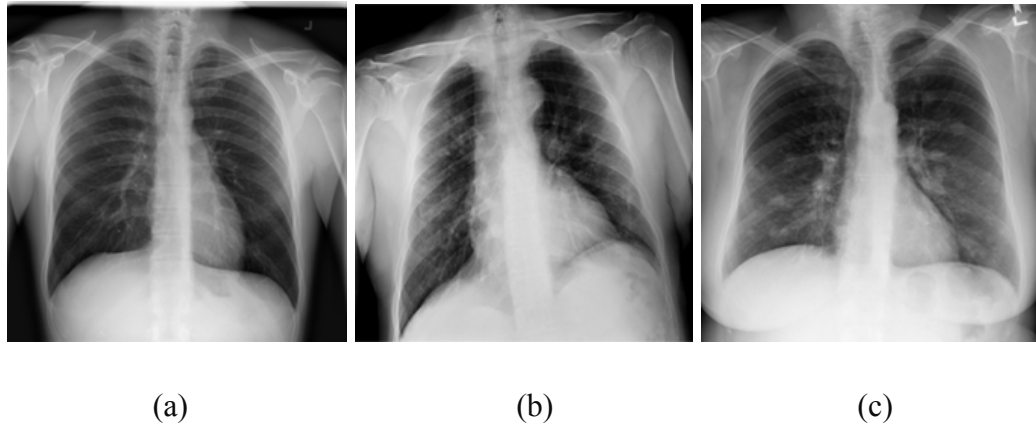


Figure 2. Samples of Covid-Qu-Ex dataset (a) Normal (b) Covid (c) Pneumonia

#### National Institute of Allergy and Infectious Diseases (NIAID) TB Dataset

Data were obtained from the TB Portals (<https://tbportals.niaid.nih.gov>), which is an open-access TB data resource supported by the National Institute of Allergy and Infectious Diseases (NIAID) Office of Cyber Infrastructure and Computational Biology (OCICB) in Bethesda, MD. These data were collected and submitted by members of the TB Portals Consortium (<https://tbportals.niaid.nih.gov/Partners>). Investigators and other data contributors who originally submitted the data to the TB Portals did not participate in the design or analysis of this study.

The institute, through its TB portals program, was able to gather linked socioeconomic/geographic, clinical, laboratory, radiological, and genomic data from over 12,900 international TB patient cases. The researchers were able to obtain 8,757 worth of chest X-ray images.



Figure 3. NIAID TB Portals dataset samples

#### Notre Dame of Dadiangas University School Clinic Data

Notre Dame of Dadiangas University, in collaboration with its school doctors, conducts medical check-ups where students must provide required clinical tests, including chest X-rays, for health assessments. However, the researchers faced difficulties as students utilized different clinics for chest X-ray diagnosis, leading to a collection of diverse images with varying quality and print standards that restricted the researchers' ability to amass a substantial volume of data of only 51 normal chest X-ray images.

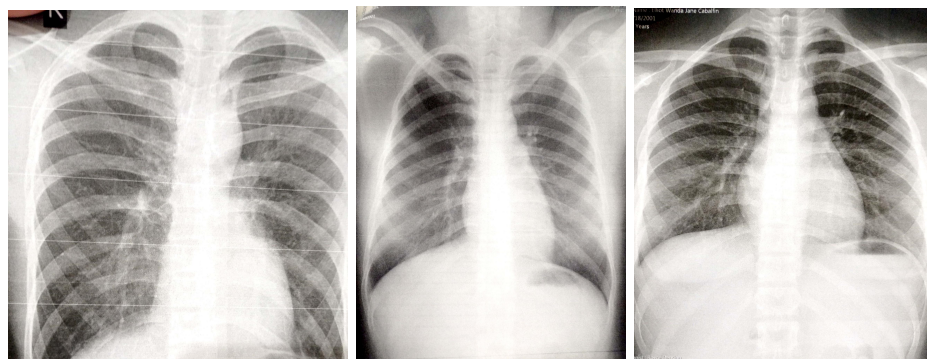


Figure 4. Notre Dame of Dadiangas University clinic data samples



Graph 1. Dataset Distribution Per Class

TABLE II. DATASET TOTAL DISTRIBUTION PER CLASS

	Normal	Pneumonia	Tuberculosis	Covid-19
Count	10, 753	11, 263	8,757	11, 956
<b>Total</b>	<b>42, 729 Chest X-Ray Images</b>			

The illustrations above show the distribution of the collected dataset per classification from reputable public online resources. The dataset was structured to meet the research objectives, merging diverse directory structures from downloaded datasets into a unified directory. Subdirectories were established for each classification category, such as Covid, Normal, Viral Pneumonia, and Bacterial Pneumonia. Using a Python script, the NIAID dataset's multiple subdirectories were combined into a single directory, and DICOM files were converted to PNG format for consistency. Despite variations in

image dimensions within the NIAID dataset, they were standardized to the model's default size (224x224 pixels) to accommodate computational limitations as shown in the figure below.

## Data Augmentation Techniques

Researchers employed various data augmentation techniques to increase the model's robustness and generalization capability based on the characteristics and domain of the dataset.

### Rescale

This function rescales the pixel values of the image by dividing them by 255 which is a form of normalization that ensures the image's pixel values to be utilized on training are within the range of 0 and 1, a recommended range preferred by neural networks (Hackers Realm, 2021).

### Shear

This function transforms an image in a slant orientation different from rotation as it slants along one axis and stretches the image in an angle specified by the value provided in a counter-clockwise direction (Kota, 2020). A value of 0.15 shear range is utilized that limits the shear as most chest X-ray (CXR) images are similar in orientation.

### Zoom

As the name implies, this function controls the range of zooming into an image based on its specified value (Hackers Realm, 2021). A value of 0.15 zoom range is

utilized that limits the zooming function as too much zooming might lose some valuable information.

### Rotation

The function rotates the image within the range specified by its value. (Hackers Realm, 2021). A value of 5 degrees is utilized to randomly rotate the images, albeit limited value, the orientation of chest X-rays is the same.

### Width Shift

The function is a decimal value ranging from 0.0 to 1.0. It indicates the maximum fraction of the total image width that can be randomly shifted either to the left or right. The shifted portion will be filled with the nearest pixel values by using the fill mode function (Sarin, 2019). A value of 0.15 is utilized as the width shift range value.

### Height Shift

The function is the same as width shift yet it shifts either at the top or bottom. The shifted portion is also filled with the nearest pixel values by using the fill mode function (Sarin, 2019). A value of 0.15 is utilized as the height shift range value.

### Brightness

This function determines the range within which a random brightness shift value is selected (Sarin, 2019). This increases the diversity of the image in terms of brightness level. 0.75 and 1.15 are values utilized as the range of brightness levels.

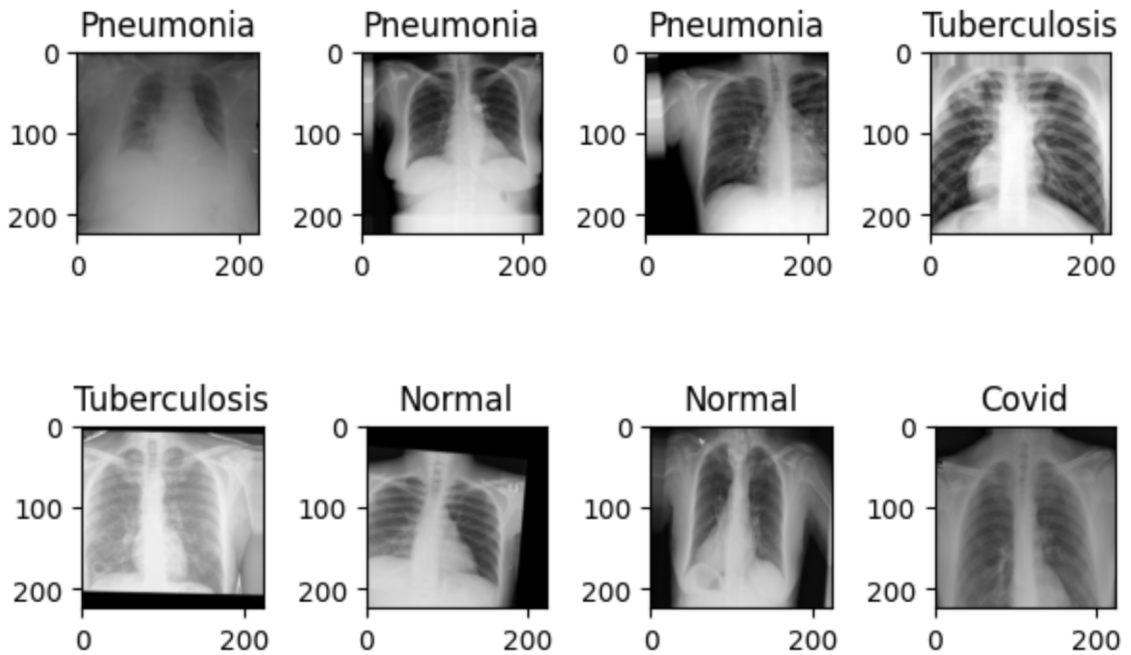


Figure 5. Dataset applied with data augmentation.

## Proposed Model Architecture

### DenseNet

An overview by Yamashita et al. stated that in recent years, deep learning has garnered significant attention from researchers. A prominent method within this domain is the Convolutional Neural Network (CNN), which proves highly effective in addressing intricate problems. Unlike conventional machine learning approaches, CNNs surpass limitations and have become widely utilized in diverse applications. Its primary advantage over predecessors lies in its ability to automatically identify significant features without human supervision, making it a preferred choice in various imaging applications (Alzubaidi et al., 2021). Its structure is designed to autonomously learn spatial hierarchies of features using a backpropagation algorithm.

DenseNet is a state-of-the-art convolutional neural network (CNN) architecture with fewer parameters for visual object recognition (Hasan et al., 2021). Within each dense block, every layer is directly connected to every other layer in a feed-forward manner. Each layer treats the feature maps of all previous layers as distinct inputs while passing on its feature maps as inputs to all layers that come after it. This network of connectivity produces cutting-edge accuracy (Huang et al., 2018). Huang et. al conducted a thorough study and introduced the architecture, and based on their benchmarks against other highly competitive object recognition tasks (CIFAR-10, CIFAR-100, SVHN, and ImageNet), DenseNet garnered massive improvements over state-of-the-art models.

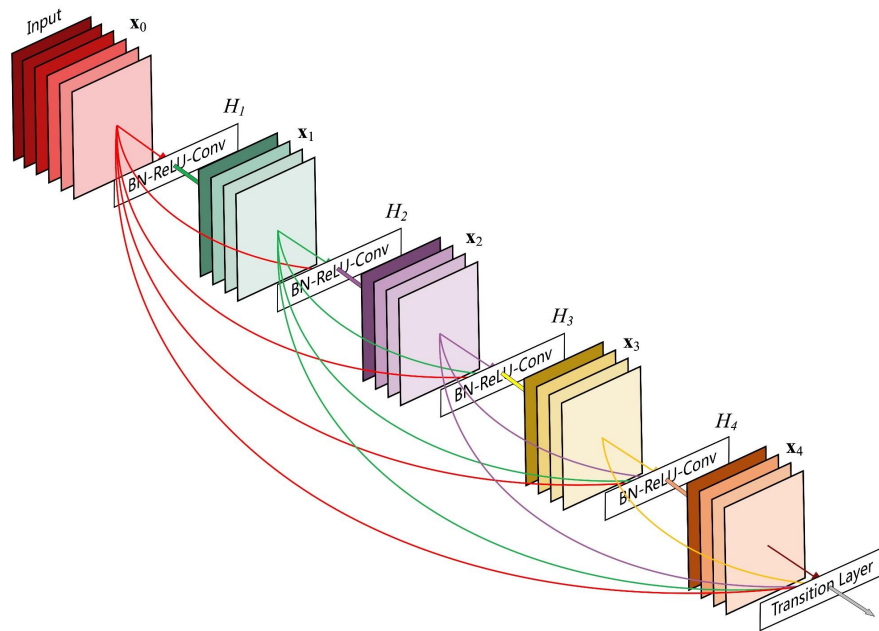


Figure 6. DenseNet model with 5 layers.

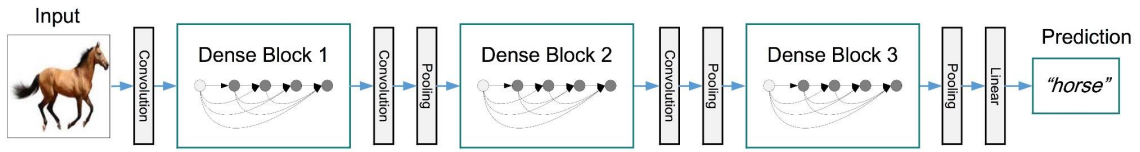


Figure 7. A DenseNet with 3 blocks.

The figures above are illustrations by Huang et. al, showcasing the structure of the DenseNet architecture. Their paper also highlighted that among their many compelling benefits, are the way the architecture mitigates the vanishing-gradient issue, enhances feature propagation, promotes feature reuse, and significantly lowers the number of parameters. The architecture proved its performance in the medical diagnosis field based on the related works presented in this paper that prompted the researchers to utilize the model.

## Transfer Learning

One of the subcategories of machine learning, transfer learning (TL), has drawn a lot of interest from the research communities in recent years (Hosna et al., 2022). Ali et al. conducted a study entitled, “Transfer Learning: A New Promising Technique”, and concluded that it is a powerful technique as it makes it possible for models to use information gained from related tasks to enhance performance on a target task which is called feature-based transfer learning. They also highlighted that based on the advancements in the machine learning industry, more and more computational resources will be consumed and that transfer learning can play a huge role in mitigating resource problems.

Due to the propagation of transfer learning, the creation of extensive open-source datasets has become imperative in the field of computer vision for many practical reasons (Antoniadis, 2022). The researchers had identified several large databases and came up with using ImageNet, a dataset where the WordNet hierarchy claimed to have 14,197, 122 manually annotated images.

### Fine-Tuning

Fine-tuning is a relevant part of this research endeavor as this research utilized transfer learning trained on ImageNet. Fine-tuning is a technique that allows us to modify an existing model that has already been trained on a particular task, utilizing the knowledge it has already gained, to accomplish a comparable task without having to start from zero (Adamson, 2022). Due to these pre-trained models having a generalized knowledge, fine-tuning allows them to adapt to a specific task (Srivastava, 2023) and allows the pre-trained model to learn a new task by removing layers that are not relevant for new information to be learned by feeding the dataset.

The researchers strategically froze the layers of the pre-trained model up to a certain point, ensuring that the foundational features learned from previous data remain fixed while training on new data. By setting these early layers as non-trainable, the model retains generalization capabilities and prevents overfitting.

Simultaneously, selectively unfreezing the last 30 layers enables the model to adapt its representations to the specific nuances of the target dataset, enhancing its ability to capture relevant features and improve overall performance in the classification task. This fine-tuning strategy optimizes the balance between leveraging existing knowledge and fine-tuning for task-specific optimization.

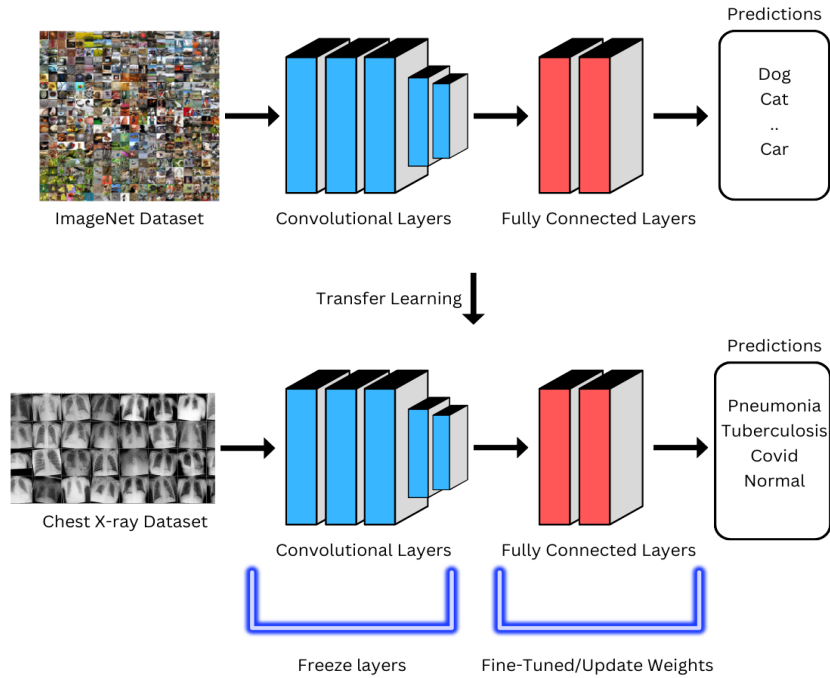


Figure 8. Transfer Learning and Fine-Tuning

### Batch Normalization

Loffe and Szegedy implied that because the parameters of the preceding layers change during training, it becomes more difficult to train deep neural networks because of this shifting input distribution for each layer. Internal Covariate Shift is the term used to describe the shift in a network's internal node's distributions during training. This known issue of deep neural networks is resolved by Batch Normalization (BN), a method for increasing the speed and stability of neural networks by dividing the result of a previous activation layer by the batch standard deviation and removing the batch mean to normalize it (Saxena, 2024).

The researchers employed batch normalization as a crucial technique in their model training process. This technique enhances the overall robustness and efficiency of

the deep learning model, making it more effective in handling complex datasets and achieving higher accuracy in classification tasks.

### Regularizations

Over recent years, overfitting is still a basic problem that hinders humans from fully generalizing the models to fit both unseen data on the testing set properly and observed data on the training sets. Overfitting occurs due to the existence of noise, the small size of the training set, and the complexity of the classifiers (Ying, 2019). Gupta, in his article, highlighted that the noise in the data points that are more likely to be random chance than the true characteristics of the data which results in lower accuracy.

The researchers added L1 and L2 regularization due to their capability to mitigate overfitting by penalizing complex models. A dropout regularization layer is also added, another regularization technique that removes a neural network's nodes. Making a new network architecture out of the parent network, all forward and backward connections with a dropped node are temporarily eliminated (Yadav, 2022).

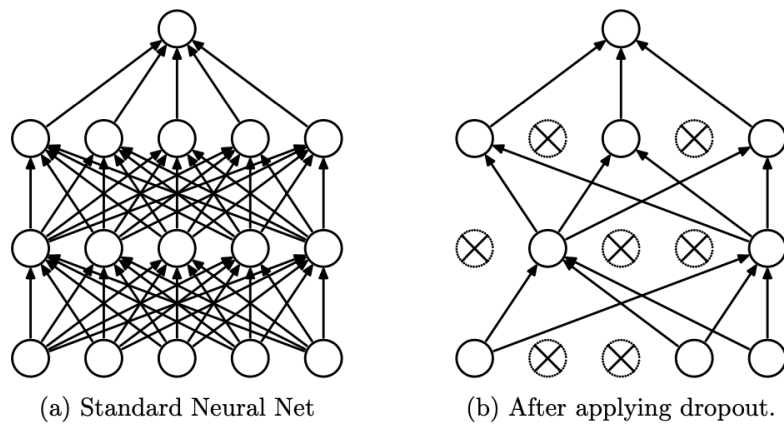


Figure 9. An Applied Dropout Layer (Srivastava et al., 2014).

The researchers incorporated additional callbacks to automate processes and enhance control during training. These callbacks include variations in learning rates over epochs, storing the best model performance, and halting training based on specific metrics (Duong, 2019). Specifically, three critical callback functions were adopted: ReduceLROnPlateau, which decreases the learning rate when performance does not improve; EarlyStopping, which stops training if improvement stalls despite learning rate adjustments; and ModelCheckpoint, which saves model weights for future use. With a k-fold cross-validation value of 5, the training and validation phases generated five models.

TABLE III. MODEL SUMMARY

Model Summary	
<b>Total Params</b>	8, 095, 300
<b>Trainable Params</b>	1, 697, 156
<b>Non-Trainable Params</b>	6, 398, 144

The model summary shown in the table above reveals 8,095,300 total parameters, with 1,697,156 trainable and 6,398,144 non-trainable parameters. This configuration aligns with the adopted approach, incorporating batch normalization, L1, and L2 regularization techniques. Notably, the fine-tuning process involved freezing all layers except the last 30, accounting for the substantial portion of non-trainable parameters derived from the pre-trained model, while the trainable parameters correspond to the fine-tuned layers adapted to the chest X-ray dataset.

## Model Evaluation

TABLE IV. CLASSIFICATION REPORT FOLD 1

	<b>Covid-19</b>	<b>Normal</b>	<b>Pneumonia</b>	<b>Tuberculosis</b>	<b>Accuracy</b>
Precision	96.26%	87.91%	89.09%	100.00%	
Recall	95.69%	88.60%	89.53%	99.20%	93%
F1-score	95.97%	88.26%	89.31%	99.60%	

TABLE V. CLASSIFICATION REPORT FOLD 2

	<b>Covid-19</b>	<b>Normal</b>	<b>Pneumonia</b>	<b>Tuberculosis</b>	<b>Accuracy</b>
Precision	95.86%	86.22%	92.67%	99.89%	
Recall	96.78%	91.67%	86.42%	99.49%	93.32%
F1-score	96.32%	88.86%	89.44%	99.69%	

TABLE VI. CLASSIFICATION REPORT FOLD 3

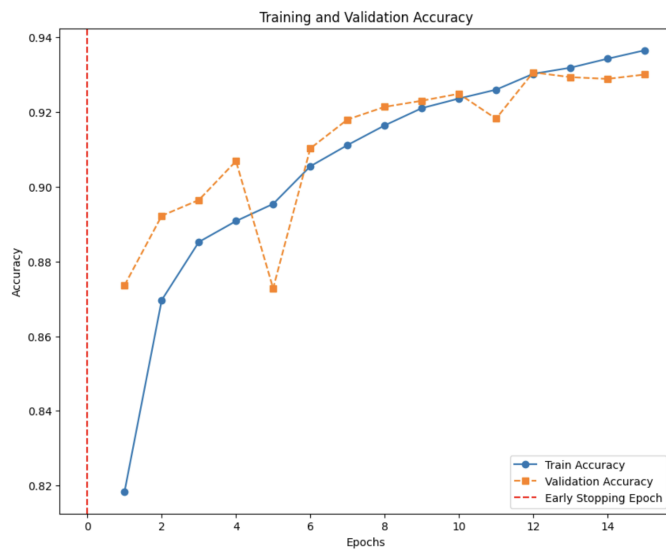
	<b>Covid-19</b>	<b>Normal</b>	<b>Pneumonia</b>	<b>Tuberculosis</b>	<b>Accuracy</b>
Precision	95.07%	85.99%	94.01%	99.60%	
Recall	96.70%	92.51%	85.62%	99.43%	93.28%
F1-score	95.87%	89.13%	89.62%	99.51%	

TABLE VII. CLASSIFICATION REPORT FOLD 4

	<b>Covid-19</b>	<b>Normal</b>	<b>Pneumonia</b>	<b>Tuberculosis</b>	<b>Accuracy</b>
Precision	96.47%	87.69%	91.67%	99.71%	
Recall	96.11%	90.47%	89.44%	99.49%	93.62%
F1-score	96.29%	89.06%	90.54%	99.60%	

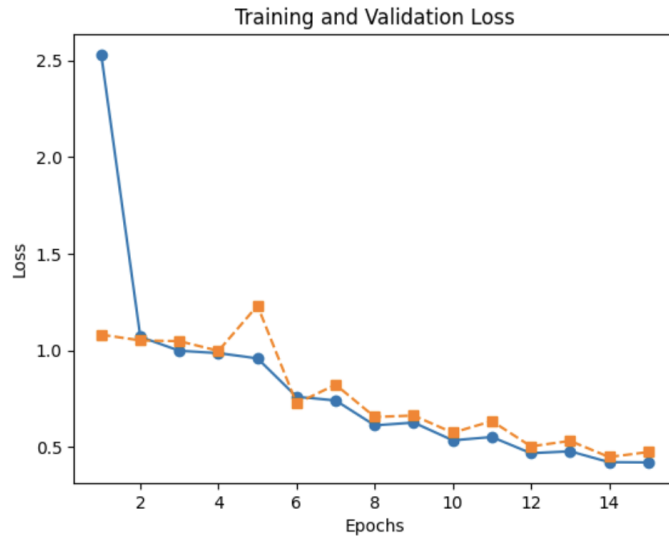
TABLE VIII. CLASSIFICATION REPORT FOLD 5

	<b>Covid-19</b>	<b>Normal</b>	<b>Pneumonia</b>	<b>Tuberculosis</b>	<b>Accuracy</b>
<b>Precision</b>	95.77%	85.13%	93.93%	99.89%	
<b>Recall</b>	96.49%	92.42%	85.89%	99.37%	93.26%
<b>F1-score</b>	96.13%	88.63%	89.73%	99.63%	



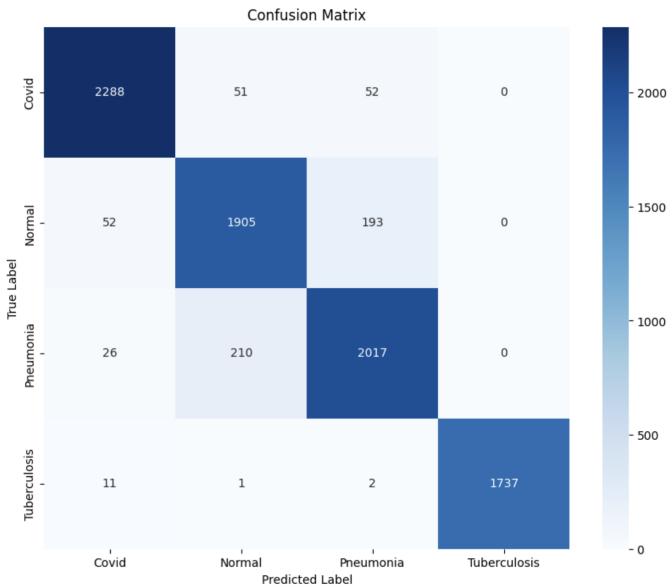
Graph 2. Model's Accuracy Plot Fold 1

Graph 2 above highlights the training and validation accuracy that presents effective learning together with good generalization of the validation set as it reaches convergence suggesting that the model was able to fit the data without any overfitting throughout 15 epochs.



Graph 3. Model's Loss Plot Fold 1

Graph 3 highlights the training and validation loss that presents effective learning due to the rapid decrease. The loss and validation loss values generally decrease across the epochs indicating that the model achieved a good fit of the data throughout 15 epochs, albeit showing signs of overfitting in the early stages.



Graph 4. Model's Confusion Matrix Fold 1

Graph 4 presents the confusion matrix achieved from Fold 1's training and validation. The model achieved remarkable results in classifying COVID-19 and Tuberculosis cases. Albeit some misclassifications, the model still performed well in classifying Normal and Pneumonia cases. Moreover, the model has shown great potential as a multi-classification system.

## Key Findings

Researchers utilized a dataset called Covid-Qu-Ex, compiled from multiple reputable online sources, containing 33,920 chest X-ray images classified into COVID-19, non-COVID infections (Viral or Bacterial Pneumonia), and Normal cases. This dataset, available on Kaggle, forms the foundation of the study. Additionally, data from the National Institute of Allergy and Infectious Diseases (NIAID) TB Dataset,

comprising 8,757 chest X-ray images, were incorporated. Challenges in data collection were faced when gathering chest X-ray images from the Notre Dame of Dadiangas University School Clinic due to variations in quality and print standards, resulting in a smaller dataset of only 51 normal chest X-ray images. Researchers employed various data augmentation techniques, including rescaling, shearing, zooming, rotation, width and height shifting, and brightness adjustment, to enhance the model's robustness and generalization. These techniques manipulate the images in ways such as adjusting orientation, zoom level, and brightness, ensuring the model's ability to learn from diverse representations of the data.

Researchers utilized DenseNet, a CNN architecture known for its efficiency and accuracy, leveraging densely connected layers within each dense block for effective feature propagation, resulting in high accuracy. They strategically froze early layers during training to preserve foundational features learned from pre-training on datasets like ImageNet, preventing overfitting and retaining generalization capabilities. Selectively unfreezing later layers allowed adaptation to target dataset nuances, enhancing classification performance. To enhance model robustness and efficiency, batch normalization stabilized and accelerated training by normalizing inputs to each layer. Additionally, L1 and L2 regularization mitigated overfitting by penalizing complex models and preventing excessively large parameter values. A dropout regularization layer was added to create diversified subnetworks, reducing overfitting risk. Employing k-fold cross-validation ensured comprehensive evaluation across the dataset, showing remarkable results from different evaluation metrics employed.

## **Chapter IV**

## **DISCUSSION**

This chapter presents an in-depth discussion of the findings, justifying the methodology employed and exploring the implications of the results. Furthermore, it acknowledges the study's limitations and proposes recommendations for future research.

### **Justification of Results**

The utilization of a comprehensive dataset encompassing various lung conditions serves as a critical foundation for evaluating the model's performance across a broad spectrum of clinical scenarios. This approach ensures that the developed model undergoes rigorous testing against real-world challenges encountered in diagnostic settings, mirroring the complexity of medical practice. By exposing the model to diverse instances of lung abnormalities, ranging from COVID-19 to pneumonia and tuberculosis, the dataset enables a thorough examination of the model's capabilities in accurately classifying chest X-ray images across different pathological conditions.

Data augmentation techniques play a pivotal role in enhancing the robustness and generalization capability of the model by diversifying the training data. By introducing controlled variations in orientation, scale, position, and illumination conditions, these techniques augment the dataset, aiding the model in learning more generalizable features and mitigating overfitting. While the augmentation strategy enriches the dataset, it's acknowledged that it may not encapsulate all possible clinical scenarios. Nonetheless, this approach complements the comprehensive dataset, ensuring that the model learns

from a broad range of variations, thereby improving its ability to classify unseen data accurately.

The strategic choice of DenseNet121 as the neural architecture, pre-trained on the ImageNet dataset, forms a robust backbone for the proposed approach. Fine-tuning this pre-trained model on the target dataset further enhances its adaptability to the specific domain, augmenting its discriminative power. Additionally, the incorporation of regularization techniques such as L1 and L2, alongside dropout and batch normalization, aims to mitigate overfitting and enhance the model's generalization capabilities. However, it's noted that without meticulous experimental fine-tuning and hyperparameter optimization, the training phase may exhibit lower results and unstable behavior, underlining the importance of rigorous model refinement processes.

The training and validation phases culminate in an overall accuracy of 93% across various respiratory conditions, underscoring the model's proficiency in classifying chest X-ray images accurately. Despite occasional fluctuations observed in the performance for normal chest X-ray images, the model consistently demonstrates high precision, recall, and F1-score values for COVID-19, pneumonia, and tuberculosis cases. This robust performance across diverse pathological conditions highlights the model's effectiveness in accurately diagnosing respiratory abnormalities, thereby holding promise for enhancing clinical decision-making and patient care.

## Implication of Results

The implications of the achieved results hold significant promise for advancing medical diagnostics and patient care in the realm of respiratory health. With an overall accuracy of 93% across various lung conditions, including COVID-19, pneumonia, and tuberculosis, the developed model showcases its potential as a reliable tool for assisting healthcare professionals in the interpretation of chest X-ray images. This high level of accuracy, particularly in identifying COVID-19 cases with precision, underscores the model's utility in aiding timely and accurate diagnosis, which is crucial for effective disease management and containment strategies.

The model's consistent performance in accurately classifying chest X-ray images across diverse pathological conditions suggests its potential for integration into clinical workflows to support healthcare decision-making. By leveraging advanced deep learning techniques and a comprehensive dataset, the model demonstrates robustness and generalizability, crucial attributes for real-world deployment in diverse healthcare settings. Its ability to reliably identify respiratory abnormalities, such as pneumonia and tuberculosis, can contribute to earlier detection and intervention, ultimately improving patient outcomes and reducing healthcare burdens.

Successful implementation of data augmentation techniques and strategic neural architecture choices highlights the importance of methodological considerations in developing accurate and reliable medical AI systems. By emphasizing rigorous experimentation and optimization processes, future endeavors in medical image analysis can build upon these findings to further enhance model performance and address

evolving healthcare challenges. This research extends beyond individual disease diagnosis, offering a glimpse into the transformative potential of AI-driven approaches in revolutionizing healthcare delivery and improving population health outcomes.

## Conclusions

Respiratory diseases like COVID-19, pneumonia, and tuberculosis pose significant challenges to public health, necessitating accurate and timely diagnostic tools. The researchers were able to develop a novel multi-classification convolutional neural network using a pre-trained DenseNet121 to classify chest X-ray images that are trained on 42,729 images from reputable public datasets. This model achieved an average accuracy of 93%, showcasing its potential as a powerful resource for healthcare professionals in aiding and enhancing diagnostic patient care.

The utilization of DenseNet121 architecture pre-trained on ImageNet, coupled with advanced techniques like transfer learning and an experimental approach for fine-tuning and hyperparameter-tuning, has led to the development of a robust and accurate model for classifying chest X-ray images. The model exhibited high precision, recall, and F1-score values for COVID-19, pneumonia, and tuberculosis cases, showcasing its effectiveness in identifying these critical diseases.

The model demonstrates promising results in the accurate classification of chest X-ray images. With further improvements, the model is a potential model for automatic diagnostic systems that aims to reduce potential human error, time-consuming manual analysis, and the potential to limit the cost of patients for additional tests that are required to confirm their illnesses. Addressing and acknowledging the limitations of this research

is vital to explore potential improvements to pave the way for more robust and reliable diagnostic models that enhance patient care.

## **Recommendations**

To further enhance the performance of the developed chest X-ray classification model, several recommendations should be considered.

1. Utilize extensive data pre-processing techniques and diverse data augmentation techniques on the dataset for better generalization capabilities.
2. Leverage high-performing GPUs such as Google Colab's premium GPUs to enable more extensive experimentation and further training of the model to unlock its full potential.
3. Collaborate with hospitals and healthcare facilities to gain access to targeted clinical datasets. This will enable the development of diagnostic systems tailored to specific healthcare facilities.
4. Incorporate the use of lung segmentation masks during model training which can help the neural network to focus on relevant regions of interest and potentially improve classification accuracy.

By implementing these recommendations, future research can build upon the promising foundation established in this study, potentially leading to more robust and reliable computer-aided diagnostic systems for respiratory diseases, ultimately improving patient outcomes and enhancing the overall quality of healthcare delivery.

## References

- Adamson, D. (2022, October 3). *Fine tuning a Convolutional Neural Network - CNN*. LinkedIn. Retrieved March 18, 2024, from <https://www.linkedin.com/pulse/fine-tuning-convolutional-neural-network-cnn-david-adamson-mbcs/>
- Agatanovic-Kustrin, S., & Beresford, R. (2000, June). Basic concepts of artificial neural network (ANN) modeling and its application in pharmaceutical research. *Journal of Pharmaceutical and Biomedical Analysis*, 22(5), 717-727. [https://doi.org/10.1016/S0731-7085\(99\)00272-1](https://doi.org/10.1016/S0731-7085(99)00272-1)
- Agusti, A., Volgemeier, C., & Halpin, D. (2022, September 23). Tackling the global burden of lung disease through prevention and early diagnosis. *The Lancet Respiratory Medicine*, 10(11), 1013-1015. [https://doi.org/10.1016/S2213-2600\(22\)00302-2](https://doi.org/10.1016/S2213-2600(22)00302-2)
- Ahmed, I. (2023, February 20). Multi-Techniques for Analyzing X-ray Images for Early Detection and Differentiation of Pneumonia and Tuberculosis Based on Hybrid Features. *Diagnostics*, 13(4), 814. doi: 10.3390/diagnostics13040814
- Ahmed, M. (2023, August 1). Joint Diagnosis of Pneumonia, COVID-19, and Tuberculosis from Chest X-ray Images: A Deep Learning Approach. *Diagnostics*, 13(5), 2562. doi: 10.3390/diagnostics13152562
- Alzubaidi, L., Zhang, J., Humaidi, A., Al-Dujaili, A., Duan, Y., Al-Shamma, O., Santamaria, J., Fadhel, M., Al-Amidie, M., & Farhan, L. (2021, March 31). Review of deep learning: concepts, CNN architectures, challenges, applications,

- future directions. *Journal of Big Data*, 8(53).
- <https://doi.org/10.1186/s40537-021-00444-8>
- An, Q., Chen, W., & Shao, W. (2024, February 11). A Deep Convolutional Neural Network for Pneumonia Detection in X-ray Images with Attention Ensemble. *Diagnostics* 2024, 14(4), 390. <https://doi.org/10.3390/diagnostics14040390>
- Antoniadis, P. (2022, November 4). *Computer Vision: Popular Datasets*. Baeldung.
- Retrieved March 18, 2024, from
- <https://www.baeldung.com/cs/computer-vision-popular-datasets>
- Ayan, E., & Ünver, H. (2019). Diagnosis of Pneumonia from Chest X-Ray Images Using Deep Learning. *2019 Scientific Meeting on Electrical-Electronics & Biomedical Engineering and Computer Science (EBBT)*, 1-5. doi: 10.1109/EBBT.2019.8741582.
- Bhatt, H., & Shah, M. (20223, November). A Convolutional Neural Network ensemble model for Pneumonia Detection using chest X-ray images. *Healthcare Analytics*, 3, 100176. <https://doi.org/10.1016/j.health.2023.100176>
- Chapter 10 - Machine learning for ARWs. (2022). In G. Nikolakopoulos, S. S. Mansouri, & C. Kanellakis (Eds.), *Aerial Robotic Workers: Design, Modeling, Control, Vision and Their Applications*. Elsevier Science.
- Cleverley, J., Piper, J., & Jones, M. (2020). The role of chest radiography in confirming covid-19 pneumonia. *BMJ*, 370. doi:10.1136/bmj.m2426
- Dadonaite, B., & Roser, M. (2019, November). *Pneumonia*. Our World in Data.
- Retrieved December 3, 2023, from <https://ourworldindata.org/pneumonia>

Dalvi, P., Edla, D., & Purushothama, B.R. (2023, February 17). Diagnosis of Coronavirus Disease From Chest X-Ray Images Using DenseNet-169 Architecture. *Advances in Computational Approaches for Image Processing, Wireless Networks, Cloud Applications and Network Security*, 4(214).

<https://doi.org/10.1007/s42979-022-01627-7>

Duong, A. (2019, August 9). *Keras Callbacks Explained In Three Minutes*. KDnuggets.

Retrieved March 18, 2024, from

<https://www.kdnuggets.com/2019/08/keras-callbacks-explained-three-minutes.html>

Flores, G., Alberto, I. R., Eala, M. A., & Canal, J. P. (2022, January). The social determinants of tuberculosis in the Philippines. *The Lancet Global Health*, 10(1), 38. [https://doi.org/10.1016/S2214-109X\(21\)00516-7](https://doi.org/10.1016/S2214-109X(21)00516-7)

Ford, L. (2023). The importance and applications of radiography in modern medicine. *J Biomed Imag Bioeng*, 7(2), 174.

<https://www.alliedacademies.org/articles/the-importance-and-applications-of-radiography-in-modern-medicine.pdf>

Goel, A., Goel, A., & Kumar, A. (2023, November 18). The role of artificial neural network and machine learning in utilizing spatial information. *Spatial Information Research*, 31(2023), 275-285. doi: 10.1007/s41324-022-00494-x

Gupta, P. (2017, November 15). *Regularization in Machine Learning | by Prashant Gupta*. Towards Data Science. Retrieved March 18, 2024, from <https://towardsdatascience.com/regularization-in-machine-learning-76441ddcf99a>

- Hackers Realm. (2021, August 21). *Data Augmentation for Image Data | Keras Tensorflow | Python*. Hackers Realm.  
<https://www.hackersrealm.net/post/data-augmentation-for-image-python>
- Hasan, N., Bao, Y., Shawon, A., & Huang, Y. (2021, July 23). DenseNet Convolutional Neural Networks Application for Predicting COVID-19 Using CT Image. *SN Computer Science*, 2(389). <https://doi.org/10.1007/s42979-021-00782-7>
- Hosna, A., Merry, E., Gyalmo, J., Alom, Z., Alom, Z., Aung, Z., & Azim, M. A. (2022, October 22). Transfer learning: a friendly introduction. *J Big Data*, 2022(9), 1. doi: 10.1186/s40537-022-00652-w
- Huang, G., Liu, Z., Maaten, L., & Weinberg, K. (2018, January 28). Densely Connected Convolutional Networks. *Computer Vision and Pattern Recognition*.  
<https://doi.org/10.48550/arXiv.1608.06993>
- Iqbal, A., Usman, M., & Ahmed, Z. (2022, September). An efficient deep learning-based framework for tuberculosis detection using chest X-ray images. *Tuberculosis*, 136. <https://doi.org/10.1016/j.tube.2022.102234>
- Islamn, E., Dawith, & Kazis. (2022, May 16). Thoracic imaging tests for the diagnosis of COVID-19. *Cochrane Database of Systematic Reviews* 2022, (5). DOI: 10.1002/14651858.CD013639.pub5.
- Ismael, A., & Sengur, A. (2021, February). Deep learning approaches for COVID-19 detection based on chest X-ray images. *Expert Systems with Applications*, 164, 114054. <https://doi.org/10.1016/j.eswa.2020.114054>
- Jain, G., Mittal, D., Thakur, D., & Mittal, M. (2020, December). A deep learning approach to detect Covid-19 coronavirus with X-Ray images. *Biocybernetics and*

- Biomedical Engineering, 40(4), 1391-1405.*  
<https://doi.org/10.1016/j.bbe.2020.08.008>
- Jain, R., Gupta, M., Taneja, S., & Hemanth, D. J. (2020, October 9). Deep learning based detection and analysis of COVID-19 on chest X-ray images. *Applied Intelligence, 51*, 1690-1700. <https://doi.org/10.1007/s10489-020-01902-1>
- Kamiri, J. (2021). Research Methods in Machine Learning: A Content Analysis. *International Journal of Computer and Information Technology, 10(2)*.  
DOI:10.24203/ijcit.v10i2.79
- Keras. (n.d.). *DenseNet*. <https://keras.io/api/applications/densenet/>
- Kota, D. K. (2020, May 17). *Understanding Image Augmentation Using Keras(Tensorflow) | by Sai Durga Kamesh Kota | Analytics Vidhya*. Medium. Retrieved March 17, 2024, from <https://medium.com/analytics-vidhya/understanding-image-augmentation-using-keras-tensorflow-a6341669d9ca>
- Kundu, R., Das, R., Geem, Z. W., Han, G.-T., & Sarkar, R. (2021, September 7). Pneumonia detection in chest X-ray images using an ensemble of deep learning models. *PLoS ONE, 16(9)*. <https://doi.org/10.1371/journal.pone.0256630>
- Loffe, S., & Szegedy, C. (2015, June). Batch Normalization: Accelerating Deep Network Training by Reducing Internal Covariate Shift. *International conference on machine learning*, 448-456.  
[https://scholar.google.com/scholar\\_lookup?arxiv\\_id=1502.03167#d=gs\\_cit&t=1710753215947&u=%2Fscholar%3Fq%3Dinfo%3A%21J8gHD1O4IJ%3Ascholar.google.com%2F%26output%3Dcite%26scirp%3D0%26hl%3Den](https://scholar.google.com/scholar_lookup?arxiv_id=1502.03167#d=gs_cit&t=1710753215947&u=%2Fscholar%3Fq%3Dinfo%3A%21J8gHD1O4IJ%3Ascholar.google.com%2F%26output%3Dcite%26scirp%3D0%26hl%3Den)

- Mohseni-Dargah, M., Falahati, Z., Dabirmanesh, B., Nasrollahi, P., & Khajeh, K. (2022). Chapter 12 - Machine learning in surface plasmon resonance for environmental monitoring. *Artificial Intelligence and Data Science in Environmental Sensingg, 2022*, 269-298. <https://doi.org/10.1016/B978-0-323-90508-4.00012-5>
- Montalbo, F. (2021, July). Diagnosing Covid-19 chest x-rays with a lightweight truncated DenseNet with partial layer freezing and feature fusion. *Biomedical Signal Processing and Control, 68*(102583). <https://doi.org/10.1016/j.bspc.2021.102583>
- Nafisah, S., & Muhammad, G. (2022, April 19). Tuberculosis detection in chest radiograph using convolutional neural network architecture and explainable artificial intelligence. *Neural Computing and Applications, 36*, 111-131. <https://doi.org/10.1007/s00521-022-07258-6>
- Nair, K., Deshpande, A., Guntuka, R., & Patil, A. (2022, April 8). Analysing X-Ray Images to Detect Lung Diseases Using DenseNet-169 technique. <https://dx.doi.org/10.2139/ssrn.4111864>
- Patel, J., & Goyal, R. (2007, September). Applications of artificial neural networks in medical science. *Curr Clin Pharmacol, 2*(3), 217-226. DOI: 10.2174/157488407781668811
- Rahman, T., Khandakar, A., & Kadir, M. (2022). Reliable Tuberculosis Detection Using Chest X-Ray With Deep Learning, Segmentation and Visualization. *IEEE Access, 8*(191586-191601). doi: 10.1109/ACCESS.2020.3031384.
- Rahman, T., Khandakar, A., Rahman, A., Zughaiier, S., Maslamani, M. A., Hossain, M., Tahir, A., Hossain, S., & Chowdhury, M. (2024, February 17). TB-CXRNet: Tuberculosis and Drug-Resistant Tuberculosis Detection Technique Using Chest

- X-ray Images. *Cognitive Computation*, 2024.  
<https://doi.org/10.1007/s12559-024-10259-3>
- Rahmati, M., Ahmadi, M., Hasanpur, S., Zare, S., Jafari, M., & Malekmohamadi. (2015). The significance of chest ultrasound and chest X-ray in the diagnosis of children clinically suspected of pneumonia. *J Med Life*, 8(3), 50-53.  
<https://www.ncbi.nlm.nih.gov/pmc/articles/PMC5348962/>
- Rajakumar, M., Sonia, R., Uma Maheswari, B., & Karuppiah, S. (2021, October 29). Tuberculosis detection in chest X-ray using Mayfly-algorithm optimized dual-deep-learning features. *IOS Press*, 29(6), 961-974. DOI: 10.3233/XST-210976
- Roger, W. (2015). Quantitative Research. *Nursing standard : official newspaper of the Royal College of Nursing*, 29(31), 44-48. doi.org/10.7748/ns.29.31.44.e8681
- Rosenthal, A., Gabrielian, A., Engle, E., Hurt, D., Alexandru, S., Crudu, V., & et al. (2017). The TB Portals: an Open-Access, Web-Based Platform for Global Drug-Resistant-Tuberculosis Data Sharing and Analysis. *J Clin Microbiol*, 55(11), 3267-82.
- Ruiz, P. (2018, October 11). *Understanding and visualizing DenseNets | by Pablo Ruiz*. Towards Data Science. Retrieved December 4, 2023, from <https://towardsdatascience.com/understanding-and-visualizing-densenets-7f688092391a>
- Ryu, Y. J. (2015, April 2). Diagnosis of Pulmonary Tuberculosis: Recent Advances and Diagnostic Algorithms. *Tuber Respir Dis*, 78(2), 64-71.  
<https://doi.org/10.4046%2Ftrd.2015.78.2.64>

- Saha, S. (2018, December 15). *A Comprehensive Guide to Convolutional Neural Networks — the ELI5 way*. Towards Data Science. Retrieved December 4, 2023, from  
<https://towardsdatascience.com/a-comprehensive-guide-to-convolutional-neural-networks-the-eli5-way-3bd2b1164a53>
- Santos, J. (2021, July 11). A REVIEW OF PNEUMONIA IN THE PHILIPPINES. *Pediatric Infectious Disease Society of the Philippines Journal*, 22(2), 6-11.  
[http://www.pidsphil.org/home/wp-content/uploads/2021/09/003\\_vol-22-no-2\\_SA\\_NTOS\\_PNEUMONIA.pdf](http://www.pidsphil.org/home/wp-content/uploads/2021/09/003_vol-22-no-2_SA_NTOS_PNEUMONIA.pdf)
- Sarin, S. (2019, October 21). *Exploring Data Augmentation with Keras and TensorFlow | by Sumit Sarin*. Towards Data Science. Retrieved March 17, 2024, from  
<https://towardsdatascience.com/exploring-image-data-augmentation-with-keras-and-tensorflow-a8162d89b844>
- Sathiratanacheewin, S., Sunanta, P., & Pongpirul, K. (2020, August 1). Deep learning for automated classification of tuberculosis-related chest X-Ray: dataset distribution shift limits diagnostic performance generalizability. *Helijon*, 6.  
<https://doi.org/10.1016/j.heliyon.2020.e04614>
- Saxena, S. (2024, February 20). *Introduction to Batch Normalization: Understanding the Basics*. Analytics Vidhya. Retrieved March 18, 2024, from  
<https://www.analyticsvidhya.com/blog/2021/03/introduction-to-batch-normalization/>

- Srivastava, N., Hinton, G., Krizhevsky, A., Sutskever, I., & Salakhutdinov, R. (2014, June). Dropout: A Simple Way to Prevent Neural Networks from Overfitting. *Journal of Machine Learning Research*, 15(2014), 1929-1956.
- Srivastava, P. (2023, July 22). *Fine-Tuning AI Models: A Guide*. *Fine-tuning is a technique for adapting... | by Prabhu Srivastava*. Medium. Retrieved March 18, 2024, from <https://medium.com/@prabhuss73/fine-tuning-ai-models-a-guide-c515bcd4b580>
- Stephen, O., Sain, M., Maduh, U., & Jeong, D.-U. (2019, March 27). An Efficient Deep Learning Approach to Pneumonia Classification in Healthcare. *Unobtrusive Sensing Technologies for the Lifecare Solution, 2019*. <https://doi.org/10.1155/2019/4180949>
- World Health Organization. (2023, November 7). *Tuberculosis*. World Health Organization (WHO). Retrieved December 3, 2023, from <https://www.who.int/news-room/fact-sheets/detail/tuberculosis>
- World Health Organization. (2023, November 22). *WHO Coronavirus Dashboard*. WHO Coronavirus (COVID-19) Dashboard | WHO Coronavirus (COVID-19) Dashboard With Vaccination Data. Retrieved December 3, 2023, from <https://covid19.who.int>
- Yadav, H. (2022, July 4). *Dropout in Neural Networks. Dropout layers have been the go-to... | by Harsh Yadav*. Towards Data Science. Retrieved March 18, 2024, from <https://towardsdatascience.com/dropout-in-neural-networks-47a162d621d9>

- Yamasahita, R., Nishio, M., Gian Do, R., & Togashi, K. (2019, June 22). Convolutional neural networks: an overview and application in radiology. *Insights into Imaging*, 9, 611-629. <https://doi.org/10.1007/s13244-018-0639-9>
- Ying, X. (2019). An Overview of Overfitting and its Solutions. *Journal of Physics: Conference Series*, 1168(2). DOI 10.1088/1742-6596/1168/2/022022
- Yue, Z., Ma, L., & Zhang, R. (2020, September 18). Comparison and Validation of Deep Learning Models for the Diagnosis of Pneumonia. *Computational and Validation of Deep Learning Models for Diagnosis of Pneumonia*, 2020. <https://doi.org/10.1155/2020/8876798>
- Zhou, T., Ye, X., Lu, H., Zhen, X., Qiu, S., & Liu, Y. (2022, April 25). Dense Convolutional Network and Its Application in Medical Image Analysis. *Microscopic Image Analysis in Histopathology*, 2022(2384830). <https://doi.org/10.1155/2022/2384830>

# APPENDICES

# **APPENDIX A**

## **Permission Letter**

## Permission Letter

**Bro Manuel De Leon**

School President

Notre Dame Dadiangas University

Dear President Bro Manuel De Leon,

I trust this letter finds you in good health. My name is Steve Vaea, a student at NDDU currently engaged in group research for my thesis. Along with my colleagues, we are writing to formally request access to the X-ray database from three, four, and five years ago at Notre Dame Dadiangas University.

The purpose of obtaining this data is to conduct a comprehensive analysis for our collective thesis, focused on Deep Learning Multi-Classification using Chest X-ray Images. The X-ray data from that period is crucial to supporting and enriching the findings of our study. I assure you that the data will be treated with the utmost care and confidentiality throughout our research process.

Understanding the significance of security and confidentiality when dealing with sensitive information, thus our commitment will align with the School Data Security Policy. Any shared information will be used strictly for academic purposes and will not be disclosed to any third party.

I kindly seek your approval to grant us access to the X-ray data for the specified timeframe. Your cooperation in this matter is pivotal for the successful completion of our group's thesis, and we genuinely appreciate your consideration of this request. I am readily available to discuss any further details or address any concerns regarding the security of the data.

Thank you for your time and consideration.

Sincerely,

**Kyle Mark Rimpos**  
Researcher

**Denrey Villamor**  
Researcher

**Steve Vaea**  
Researcher

**Mrs. Lorelyn Adrales, MCS, MBA**  
Thesis Adviser

**Engr. Shiela Sorino, MEE-CE**  
CEAT DEAN

**Br. Manuel V. de Leon**  
University President

# **APPENDIX B**

## **Research Timetable**

#### TABLE IX. RESEARCH TIMETABLE

# **APPENDIX C**

## **Training And Validation**

### **Data**

TABLE X. TRAINING AND VALIDATION DATA FOLD 1

Epoch	Loss	Accuracy	Val_Loss	Val_Accuracy	Learning_Rate
1	2.5289	0.8184	1.0813	0.8736	0.0010
2	1.0702	0.8696	1.0515	0.8922	0.0010
3	0.9980	0.8852	1.0477	0.8964	0.0010
4	0.9860	0.8908	0.9976	0.9068	0.0010
5	0.9587	0.8954	1.2315	0.8728	0.0007
6	0.7603	0.9055	0.7254	0.9102	0.0007
7	0.7411	0.9111	0.8228	0.9180	0.00049
8	0.6126	0.9164	0.6559	0.9214	0.00049
9	0.6267	0.9210	0.6630	0.9230	0.000343
10	0.5350	0.9236	0.5743	0.9249	0.000343
11	0.5522	0.9260	0.6346	0.9182	0.000240
12	0.4683	0.9302	0.5038	0.9306	0.000240
13	0.4785	0.9318	0.5322	0.9293	0.000168
14	0.4223	0.9342	0.4488	0.9288	0.000168
15	0.4211	0.9365	0.4742	0.9300	0.000118

Table X shows the training and validation data for fold 1 across 15 epochs. The loss and validation loss values generally decrease over epochs, while accuracy and validation accuracy increase, indicating the model is improving its performance on both the training and validation data. The learning rate remains mostly constant except for small decreases towards the later epochs.

TABLE XI. TRAINING AND VALIDATION DATA FOLD 2

Epoch	Loss	Accuracy	Val_Loss	Val_Accuracy	Learning_Rate
1	2.5244	0.8184	1.1523	0.8689	0.0010
2	1.0668	0.8703	1.3296	0.8705	0.0007
3	0.8152	0.8913	0.8206	0.8981	0.0007
4	0.7747	0.8993	0.8665	0.9092	0.00049
5	0.6520	0.9086	0.6595	0.9174	0.00049
6	0.6453	0.9143	0.7696	0.8919	0.000343
7	0.5519	0.9217	0.6315	0.9204	0.000343
8	0.5779	0.9222	0.6231	0.9217	0.000343
9	0.5876	0.9235	0.6035	0.9231	0.000343
10	0.5709	0.9277	0.6130	0.9251	0.000240
11	0.4838	0.9314	0.5429	0.9251	0.000240
12	0.4863	0.9320	0.5224	0.9263	0.000240
13	0.4795	0.9348	0.5647	0.9197	0.000168
14	0.4164	0.9368	0.4472	0.9304	0.000168
15	0.4229	0.9380	0.4576	0.9332	0.000118

Table XI shows the training and validation data for fold 2 across 15 epochs. Similar to fold 1, the loss and validation loss values generally decrease, while the accuracy and validation accuracy increase as the number of epochs progresses. The learning rate is initially higher but decreases in later epochs. The trends indicate that the model is learning and improving its performance on both the training and validation data for this specific data fold throughout the training process.

TABLE XII. TRAINING AND VALIDATION DATA FOLD 3

Epoch	Loss	Accuracy	Val_Loss	Val_Accuracy	Learning_Rate
1	2.5474	0.8171	1.2672	0.8356	0.0010
2	1.0681	0.8686	1.0985	0.8976	0.0010
3	1.0905	0.8754	1.0804	0.8671	0.0010
4	1.0214	0.8859	1.1971	0.8577	0.0007
5	0.7762	0.8992	0.8265	0.9162	0.0007
6	0.7665	0.9049	0.8085	0.9119	0.0007
7	0.7890	0.9090	0.8247	0.9098	0.00049
8	0.6482	0.9138	0.6872	0.9224	0.00049
9	0.6804	0.9153	0.7128	0.9150	0.000343
10	0.5406	0.9233	0.5625	0.9188	0.000343
11	0.5504	0.9251	0.6243	0.9255	0.000240
12	0.4773	0.9286	0.5062	0.9285	0.000240
13	0.4677	0.9319	0.5003	0.9281	0.000240
14	0.4860	0.9317	0.5672	0.9219	0.000168
15	0.4236	0.9351	0.4540	0.9328	0.000168

Table XII shows the training and validation data for fold 3 across 15 epochs. Similar to the previous folds, the loss and validation loss generally decrease, while the accuracy and validation accuracy increase over the epochs, indicating the model is improving its performance on both the training and validation data for this specific data fold. The learning rate follows a comparable pattern, starting higher and decreasing slightly in later epochs.

TABLE XIII. TRAINING AND VALIDATION DATA FOLD 4

Epoch	Loss	Accuracy	Val_Loss	Val_Accuracy	Learning_Rate
1	2.4970	0.8188	1.3504	0.8049	0.0010
2	1.0783	0.8688	1.0978	0.8860	0.0010
3	0.9936	0.8846	1.0850	0.8770	0.0010
4	0.9662	0.8908	1.0413	0.8929	0.0010
5	0.9204	0.8971	1.0368	0.9100	0.0010
6	0.9052	0.9000	1.0480	0.8877	0.0007
7	0.7234	0.9101	0.7262	0.9228	0.0007
8	0.7517	0.9142	0.7790	0.9129	0.00049
9	0.6021	0.9210	0.6302	0.9219	0.00049
10	0.6108	0.9231	0.6907	0.9194	0.000343
11	0.5165	0.9267	0.5291	0.9262	0.000343
12	0.5290	0.9289	0.5617	0.9242	0.000240
13	0.4401	0.9324	0.4561	0.9300	0.000240
14	0.4525	0.9336	0.5149	0.9267	0.000168
15	0.4041	0.9372	0.4169	0.9362	0.000168

Table XIII shows the training and validation data for fold 4 across 15 epochs. In line with previous iterations, there's a consistent trend of decreasing loss and validation loss, alongside increasing accuracy and validation accuracy across epochs. This indicates a continual enhancement in the model's performance on both training and validation data within this particular data fold. Moreover, the learning rate displays a similar pattern, initially higher before gradually decreasing in subsequent epochs.

TABLE XIV. TRAINING AND VALIDATION DATA FOLD 5

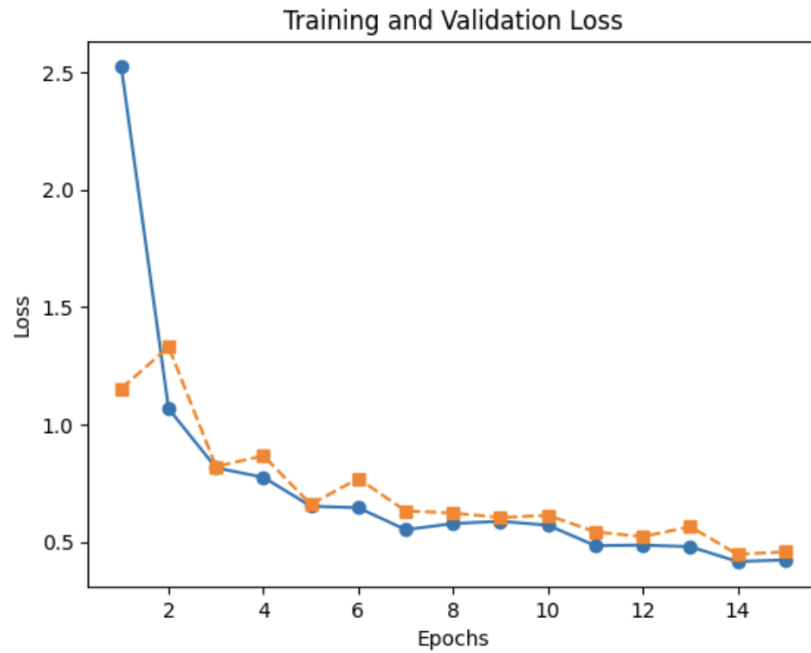
Epoch	Loss	Accuracy	Val_Loss	Val_Accuracy	Learning_Rate
1	2.5255	0.8180	1.1841	0.8734	0.0010
2	1.0944	0.8675	1.0868	0.8910	0.0010
3	1.0415	0.8790	1.0118	0.9018	0.0010
4	0.9941	0.8856	1.0470	0.9030	0.0007
5	0.7484	0.9013	0.8053	0.9088	0.0007
6	0.7547	0.9060	0.8243	0.9088	0.00049
7	0.6406	0.9123	0.7358	0.9130	0.00049
8	0.6510	0.9167	0.7586	0.9155	0.000343
9	0.5398	0.9227	0.5812	0.9203	0.000343
10	0.5715	0.9239	0.6032	0.9260	0.000240
11	0.4667	0.9297	0.5486	0.9222	0.000240
12	0.4841	0.9306	0.5516	0.9259	0.000168
13	0.4182	0.9348	0.5022	0.9235	0.000168
14	0.4298	0.9337	0.4808	0.9274	0.000168
15	0.4417	0.9340	0.4691	0.9326	0.000168

Table XIII shows the training and validation data for fold 4 across 15 epochs. Much like in previous instances, there's a consistent pattern where the loss and validation loss steadily decrease, while accuracy and validation accuracy progressively rise throughout the epochs. This trend suggests an ongoing improvement in the model's performance across both training and validation datasets within this specific fold. Additionally, the learning rate exhibits a similar trajectory, starting relatively high and then gradually declining as training progresses. Between using different subsets of the

dataset as training and validation data, it showed remarkable consistency indicating that the model can predict new, unseen data.

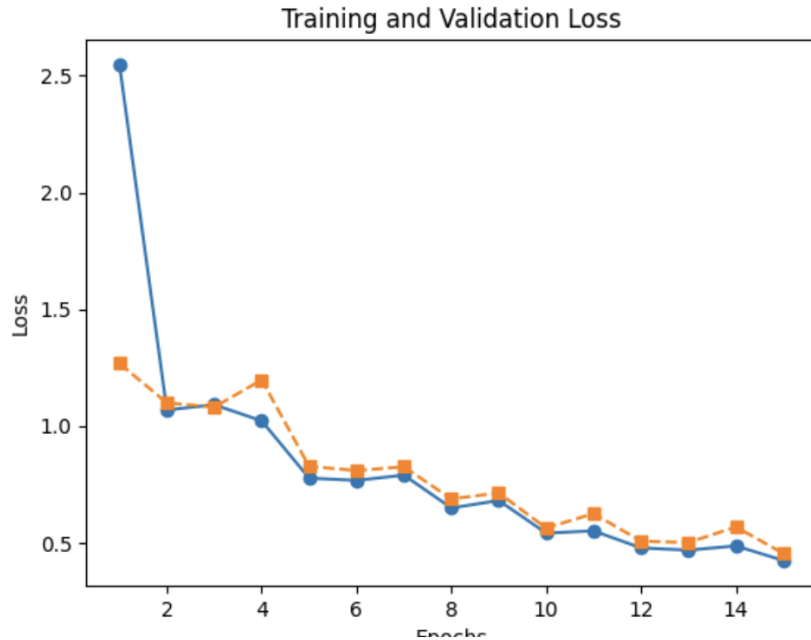
# **APPENDIX D**

## **Loss Plot**



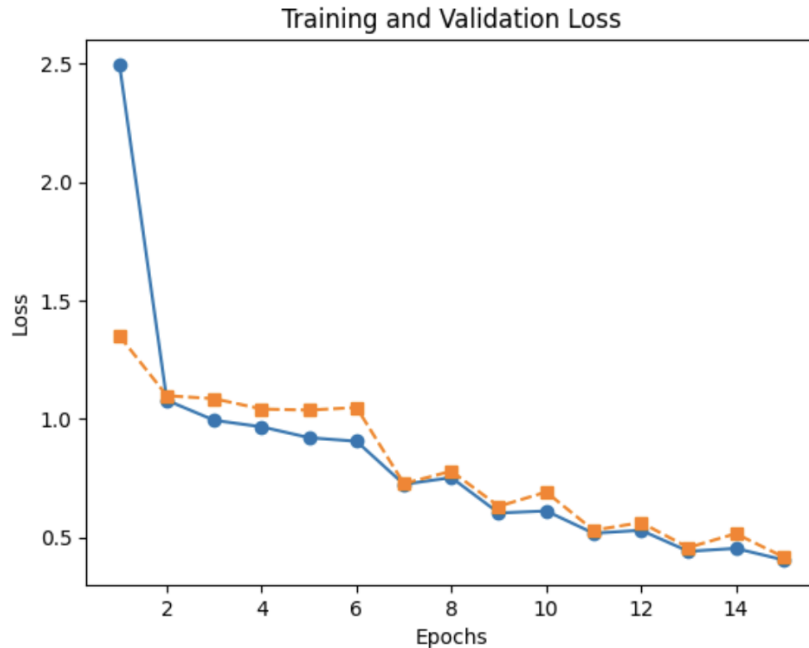
Graph 5. Model's Loss Plot Fold 2

Graph 5 shows the training and validation loss of fold 2 across 15 epochs. The plot shows a decreasing trend and a minimal gap as the training progresses.



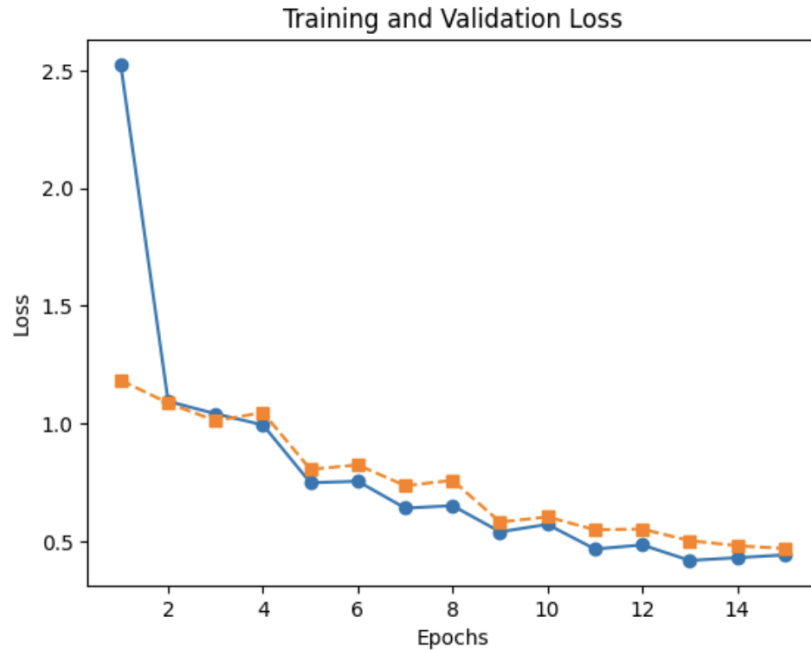
Graph 6. Model's Loss Plot Fold 3

Graph 6 shows the training and validation loss of fold 3 across 15 epochs. Similar to fold 2, the plot shows a decreasing trend and a minimal gap as the training progresses.



Graph 7. Model's Loss Plot Fold 4

Graph 7 shows the training and validation loss of fold 4 across 15 epochs. Similar to the previous folds, the plot shows a decreasing trend and a minimal gap as the training progresses.

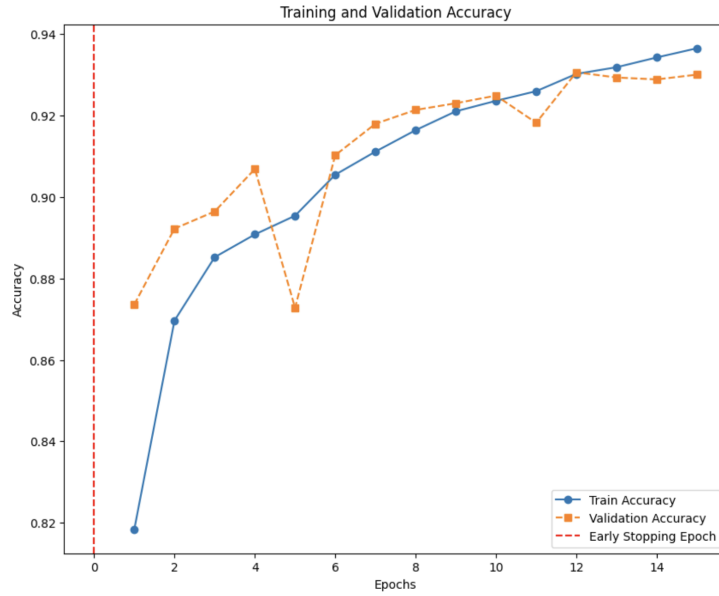


Graph 8. Model's Loss Plot Fold 5

Graph 8 shows the training and validation loss of fold 5 across 15 epochs. Similar to all the previous folds, the plot shows a decreasing trend and a minimal gap as the training progresses. All folds show similar patterns where in the early stages of the training.

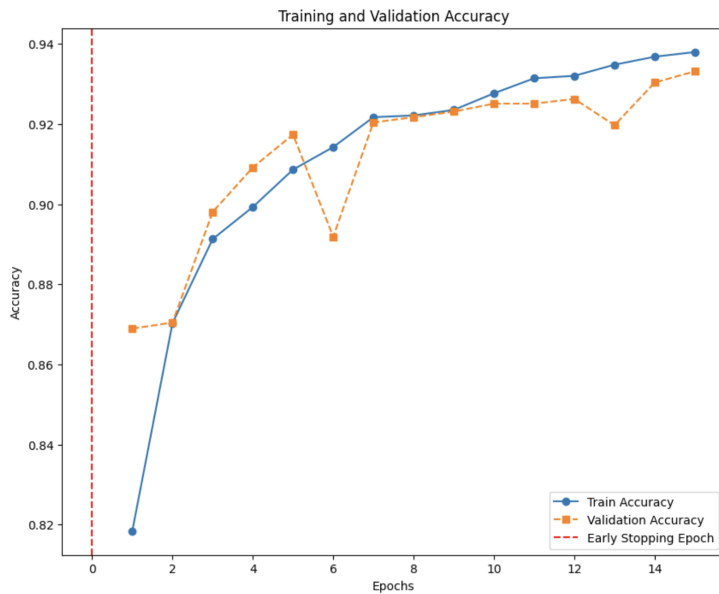
# **APPENDIX E**

## **Accuracy Plot**



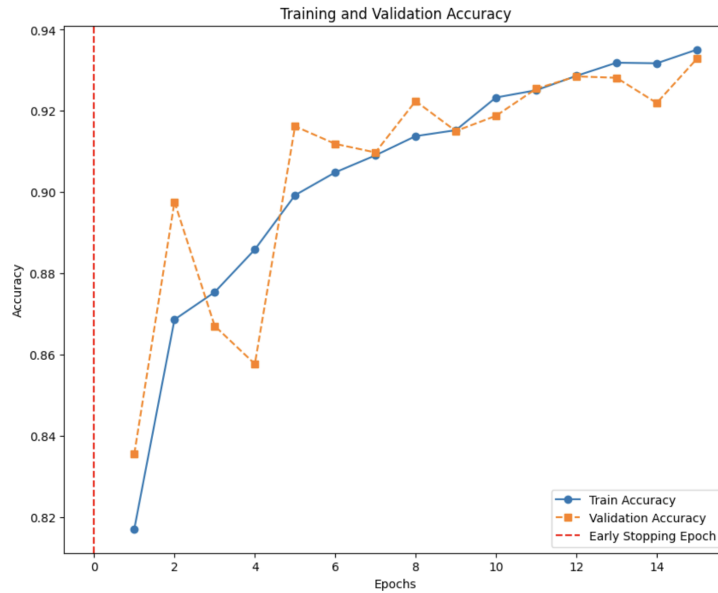
Graph 9. Mode's Accuracy Plot Fold 2

Graph 9 shows the training and validation accuracy of fold 2 over 15 epochs. The training accuracy improves rapidly, while the validation accuracy lags in the early stages, indicating signs of overfitting. However, as the learning rate is reduced, validation accuracy improves suggesting effective learning. Early stopping, did not activate in this fold.



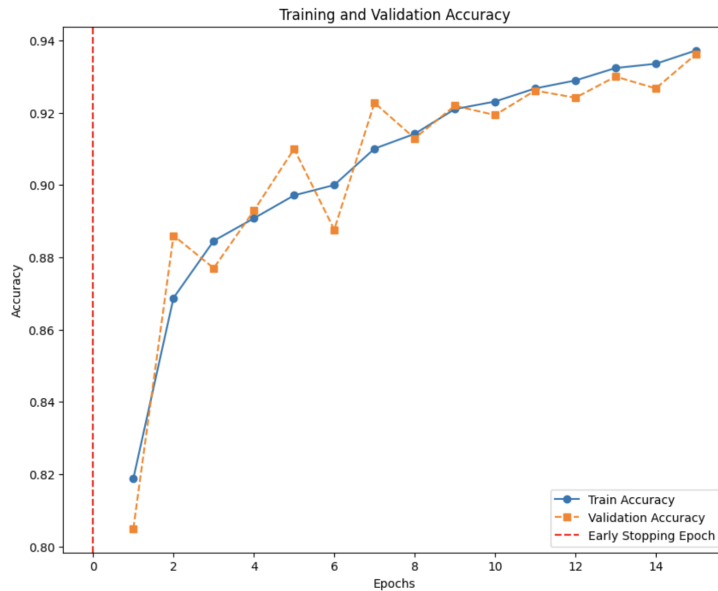
Graph 10. Model's Accuracy Plot Fold 3

Graph 10 shows the training and validation accuracy of fold 3 over 15 epochs. The training accuracy also improves rapidly, while the validation accuracy lags in the early stages, indicating signs of overfitting. However, as the learning rate is also being reduced, validation accuracy improves suggesting effective learning. Early stopping, did not activate in this fold.



Graph 11. Model's Accuracy Plot Fold 4

Graph 11 shows the training and validation accuracy of fold 4 over 15 epochs. The training accuracy improves rapidly like the previous folds, while the validation accuracy lags in the early stages, indicating signs of overfitting. However, as the learning rate is also being reduced, validation accuracy improves suggesting effective learning leading to convergence. Early stopping, did not activate in this fold.

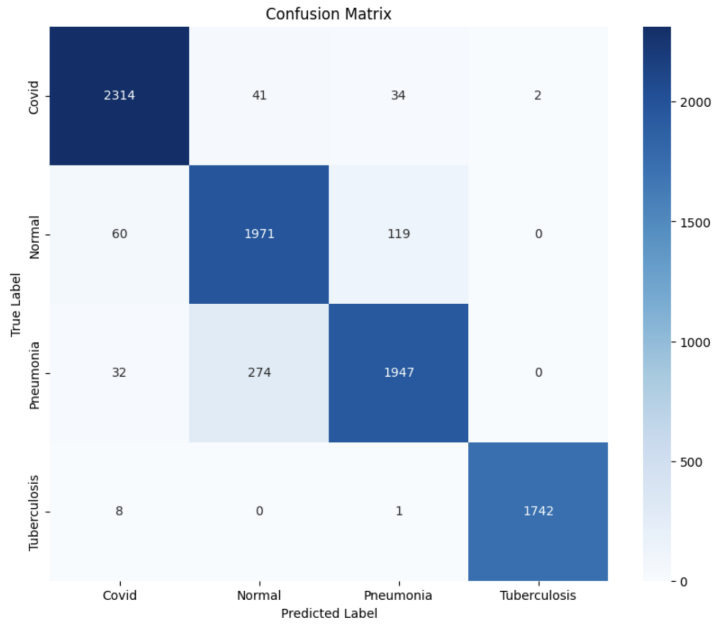


Graph 12. Model's Accuracy Plot Fold 5

Graph 12 shows the training and validation accuracy of fold 5 over 15 epochs. The training accuracy has been consistent with its previous folds, while the validation accuracy lags in the early stages, indicating signs of overfitting. However, as the learning rate is also being reduced, validation accuracy improves suggesting effective learning leading to convergence.

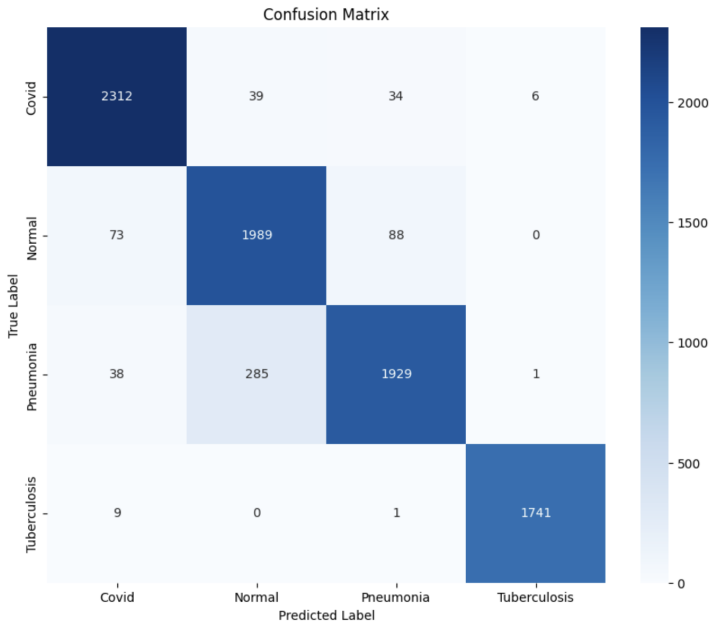
# **APPENDIX F**

## **Confusion Matrix**



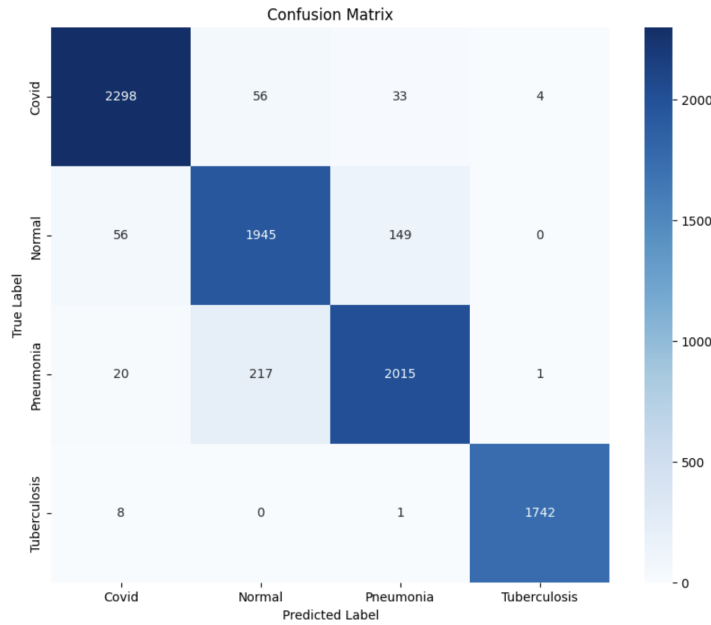
Graph 13. Model's Confusion Matrix Fold 2

Graph 13 presents the confusion matrix achieved from Fold 2's training and validation. The model achieved remarkable results in classifying COVID-19 and Tuberculosis cases. Albeit some misclassifications, the model still performed well in classifying Normal and Pneumonia cases.



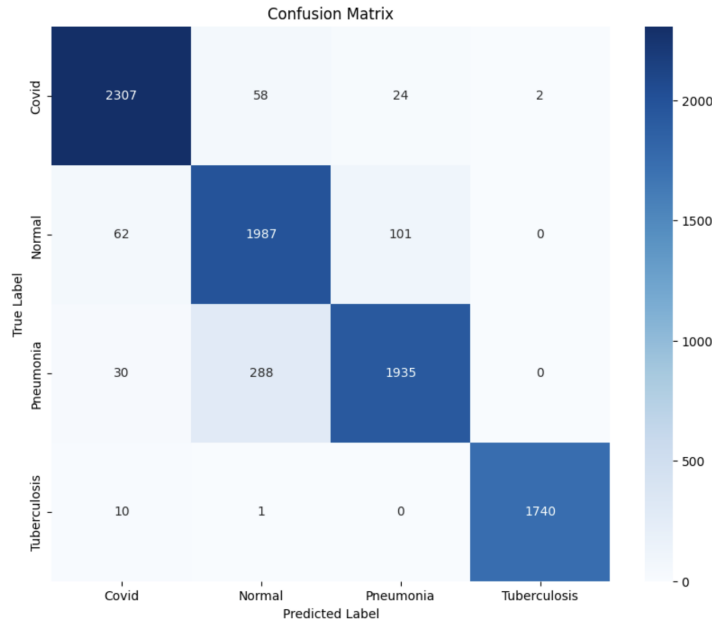
Graph 14. Model's Confusion Matrix Fold 3

Graph 14 presents the confusion matrix achieved from Fold 3's training and validation. The model achieved the same remarkable results with fold 1 in classifying COVID-19 and Tuberculosis cases. Albeit some misclassifications, the model still performed well in classifying Normal and Pneumonia cases.



Graph 15. Model's Confusion Matrix Fold 4

Graph 15 presents the confusion matrix achieved from Fold 4's training and validation. The model achieved the same remarkable results as the previous results in classifying COVID-19 and Tuberculosis cases. Albeit some misclassifications, the model still performed well in classifying Normal and Pneumonia cases.



Graph 16. Model's Confusion Matrix Fold 5

Graph 16 presents the confusion matrix achieved from Fold 5's training and validation. The model achieved the same remarkable results as the previous results in classifying COVID-19 and Tuberculosis cases. Albeit some misclassifications, the model still performed well in classifying Normal and Pneumonia cases. Moreover, all achieved remarkable results highlighting its potential in chest X-ray diagnostics.

# **APPENDIX G**

# **Curriculum Vitae**

**Denrey M. Villamor**

Malandag, Malungon, Sarangani, Province  
09669183079  
denreyvillamor05@gmail.com

**PERSONAL DATA**

Date of Birth: February 23, 2002	Civil Status: Single
Place of Birth: Malandag, Malungon, Sarangani, Province	Citizenship: Filipino
Age: 21	Sex: Male
Religion: Members Church of God International	Height: 170.7 cm
Weight: 86 kg	

**SKILLS**

- Coding Languages: Familiar with C++ and Visual Basic programming language
- Information Gathering: Competent in gathering and organizing information effectively
- Attention to Detail: Attentive to identifying errors and inconsistencies
- Technical Writing: Proficient in explaining technical concepts clearly and concisely
- Team Collaboration: Collaborative and supportive team member
- Computer Hardware: Basic knowledge with a strong willingness to learn and expand skills

**AFFILIATIONS**

- Philippine Society of Information Technology Students

Member (2020-Present)

- Peer Facilitator

Member (2023-Present)

**EDUCATIONAL ATTAINMENT**

- Tertiary      Notre Dame of Dadiangas University

Marist Avenue General Santos City  
Bachelor of Science in Computer Science  
S.Y 2020 – Present

- Secondary Notre Dame of Dadiangas University

Marist Avenue General Santos City  
Science, Technology, Engineering & Mathematics  
S.Y 2018 – 2020  
Malandag Adventist Academy inc.  
Malandag, Malungon, Sarangani, Province  
S.Y 2014-2018

- Elementary Malandag Adventist Academy inc.

Malandag, Malungon, Sarangani, Province  
S.Y 2008-2014

## EXPERIENCE

- CMO-ICTD  
General Santos City  
ON-THE-JOB TRANIEE  
240 Hr.  
2023
- NDDU – Computer Laboratory  
General Santos City  
JOB IMMERSION  
80 Hr.  
2018

## Kyle Mark Rimpos

City Heights, General Santos City  
09278224007  
denreyvillamor05@gmail.com



### PERSONAL DATA

Date of Birth: July 28, 2000	Civil Status: Single
Place of Birth: General Santos City	Citizenship: Filipino
Age: 23	Sex: Male
Religion: Roman Catholic	Height: 167.7 cm
Weight: 84 kg	

### SKILLS

- Web Development
- Python, C++, Java,
- OOP
- Office Tools (Microsoft Office, Google Suite)
- Data Analysis
- Web Scraping
- Teamwork
- Machine Learning
- Attention to detail
- Adaptability
- Communication and Presentation
- Leadership
- Critical Thinking

### AFFILIATIONS

- Philippine Society of Information Technology Students
  - Club Treasurer (2023 - 2024)
  - Club Member (2021 - 2023)

### EDUCATIONAL ATTAINMENT

- Notre Dame of Dadiangas University
    - Marist Avenue General Santos City
    - Bachelor of Science in Computer Science
- S.Y 2020 – Present

- Notre Dame-Siena College of General Santos City
  - Science, Technology, Engineering & Mathematics S.Y 2007 – 2019

## **EXPERIENCE**

- Supply Chain Project Intern
  - Cannery Site, Polomolok, South Cotabato

## Steve Sefo Vaea

Mauga Savai'i Samoa (Western Samoa)  
09286984244 / 095669996096  
20brstevevaea19@gmail.com



### PERSONAL DATA

<b>Date of Birth:</b> March 21, 1995	<b>Civil Status:</b> Single
<b>Place of Birth:</b> Mauga, Savai'i Samoa	<b>Citizenship:</b> Samoan
<b>Age:</b> 29	<b>Sex:</b> Male
<b>Religion:</b> Roman Catholic Church	<b>Height:</b> 175 cm
<b>Weight:</b> 105 kg	

### SKILLS

- Communication skills: Effective communication both verbal and written.
- Coding Languages: Familiar with C++ and Visual Basic programming language
- Operating systems, including processes, memory management, file systems, and networking, is essential for developing system-interacting software.
- Basic Knowledge for Computer Hardware

### AFFILIATIONS

- **Philippine Society of Information Technology Students**

Member (2021-Present)

- **Joint Photographic Group**

Member (2023-Present)

### EDUCATIONAL ATTAINMENT

- National University of Samoa
  - To'omata'agi, Apia Samoa
  - Bachelor of Science
- Institute of Formation and Religious Studies
  - S.Y 2014 – 2016 (inc)
  - S.Y 2019 – 2020

- Marist Asia and Pacific Formation Center S.Y 2019 – 2020
- Notre Dame of Dadiangas University
  - Marist Avenue General Santos City
  - Bachelor of Science in Computer Science S.Y 2021 – Present
- Tuasivi College
  - Savai'i, Samoa
  - Physic Science, Computer Study, English & Mathematics S.Y 2009 – 2013
- Samalaeulu Primary School
  - Savai'i Samoa S.Y 2021 - 2008

## EXPERIENCE

- **DOLE PHILIPPINES, INC**

**Quality Assurance in the IT and Application Department**

Polomolok, South Cotabato

**ON-THE-JOB TRAINEE**

240 Hr.

2023